AMERICAN SOCIETY FOR MICROBIOLOGY | Journal of Bacteriology®

RESEARCH ARTICLE

The Mutant β^{E202K} Sliding Clamp Protein Impairs DNA Polymerase III Replication Activity

Caleb Homiski,[a] Michelle K. Scotland,[a] Vignesh M. P. Babu,[a]* Sundari Chodavarapu,[b]§ Robert W. Maul,[a]◊ Jon M. Kaguni,[b] Mark D. Sutton[a]

[a]Department of Biochemistry, Jacobs School of Medicine and Biomedical Sciences, University at Buffalo, State University of New York, Buffalo, New York, USA
[b]Department of Biochemistry and Molecular Biology, Michigan State University, East Lansing, Michigan, USA

Caleb Homiski and Michelle K. Scotland contributed equally to this work. Author order was determined alphabetically.

ABSTRACT Expression of the *Escherichia coli dnaN*-encoded β clamp at ≥10-fold higher than chromosomally expressed levels impedes growth by interfering with DNA replication. We hypothesized that the excess β clamp sequesters the replicative DNA polymerase III (Pol III) to inhibit replication. As a test of this hypothesis, we obtained eight mutant clamps with an inability to impede growth and measured their ability to stimulate Pol III replication *in vitro*. Compared with the wild-type clamp, seven of the mutants were defective, consistent with their elevated cellular levels failing to sequester Pol III. However, the β^{E202K} mutant that bears a glutamic acid-to-lysine substitution at residue 202 displayed an increased affinity for Pol IIIα and Pol III core (Pol III$\alpha\varepsilon\theta$), suggesting that it could still sequester Pol III effectively. Of interest, β^{E202K} supported *in vitro* DNA replication by Pol II and Pol IV but was defective with Pol III. Genetic experiments indicated that the *dnaN*^{E202K} strain remained proficient in DNA damage-induced mutagenesis but was induced modestly for SOS and displayed sensitivity to UV light and methyl methanesulfonate. These results correlate an impaired ability of the mutant β^{E202K} clamp to support Pol III replication *in vivo* with its *in vitro* defect in DNA replication. Taken together, our results (i) support the model that sequestration of Pol III contributes to growth inhibition, (ii) argue for the existence of an additional mechanism that contributes to lethality, and (iii) suggest that physical and functional interactions of the β clamp with Pol III are more extensive than appreciated currently.

IMPORTANCE The β clamp plays critically important roles in managing the actions of multiple proteins at the replication fork. However, we lack a molecular understanding of both how the clamp interacts with these different partners and the mechanisms by which it manages their respective actions. We previously exploited the finding that an elevated cellular level of the β clamp impedes *Escherichia coli* growth by interfering with DNA replication. Using a genetic selection method, we obtained novel mutant β clamps that fail to inhibit growth. Their analysis revealed that β^{E202K} is unique among them. Our work offers new insights into how the β clamp interacts with and manages the actions of *E. coli* DNA polymerases II, III, and IV.

KEYWORDS DNA polymerase, DNA replication, fidelity, mutagenesis, sliding clamp, protein-protein interactions

The *Escherichia coli dnaN* gene encodes a 366-amino acid (40.6 kDa) protein that homodimerizes to adopt a closed, ring-like structure referred to as the β sliding clamp (1–3). In its active form, the β clamp encircles double-stranded DNA (dsDNA) to tether a number of partner proteins to the DNA, granting them access to their sites of action, and in at least some cases, enhancing their catalytic activity (reviewed in reference 4). The β clamp is loaded onto DNA by the 7-subunit ATPase referred to as the

Citation Homiski C, Scotland MK, Babu VMP, Chodavarapu S, Maul RW, Kaguni JM, Sutton MD. 2021. The mutant β^{E202K} sliding clamp protein impairs DNA polymerase III replication activity. J Bacteriol 203:e00303-21. https://doi.org/10.1128/JB.00303-21.

Editor Thomas J. Silhavy, Princeton University

Address correspondence to Mark D. Sutton, mdsutton@buffalo.edu.

*Present address: Vignesh M. P. Babu, Department of Biology, Massachusetts Institute of Technology, Cambridge, Massachusetts, USA.

§Present address: Sundari Chodavarapu, Nivagen Pharmaceuticals, Inc., Davis, California, USA.

◊Present address: Robert W. Maul, Laboratory of Molecular Biology and Immunology, National Institute on Aging, National Institutes of Health, Baltimore, Maryland, USA.

For a companion article on this topic, see https://doi.org/10.1128/JB.00304-21.

Received 2 June 2021
Accepted 11 September 2021
Accepted manuscript posted online 20 September 2021
Published 5 November 2021

DnaX clamp loader complex (5, 6). The DnaX complex consists of 3 copies of the ATP-binding *dnaX* gene product, which undergoes a programmed translational frameshift to produce the full-length τ protein, or the C-terminally truncated γ protein (7), together with 1 copy each of δ, δ', χ, and ψ (8, 9). The DnaX-ATP_3-β complex binds to a dsDNA/single-strand DNA (ssDNA) junction (reviewed in reference 10), with a strong preference for the 3′-OH end of the dsDNA/ssDNA junction (11). Once bound to DNA, DnaX hydrolyzes bound ATP triggering the release of the β clamp and the subsequent dissociation of DnaX from the DNA, leaving behind the clamp assembled on dsDNA. Nucleotide sequence-independent β clamp-DNA interactions contribute to loading (1, 12) and, to a lesser extent, certain clamp functions on DNA, including the ability of *E. coli* to cope with DNA damage (12, 13).

The β clamp was identified initially as the processivity subunit of the 17-subunit bacterial replicase DNA polymerase III (Pol III) holoenzyme (HE) (3, 14). At the replication fork, Pol III HE consists of the following subassemblies: the DnaX complex ($DnaX_3\delta\delta'\chi\psi$), 2 Pol III catalytic core complexes (Pol III$\alpha\varepsilon\theta$) with both polymerase (Pol IIIα) and 3′-to-5′ exonuclease proofreading activity (Pol III$\varepsilon\theta$), and 2 homodimeric β clamps (reviewed in references 15 and 16). In the absence of the β clamp, Pol III is largely distributive, incorporating on average 10 to 20 nucleotides per DNA binding event. However, in the presence of the β clamp, the DnaX complex, and additional accessory replication proteins, Pol III becomes highly processive (17). Its extreme processivity is mediated by contacts between the α and ε subunits of Pol III and the β clamp (18–20).

Of interest, the β clamp interacts functionally with many other proteins. They include the DnaX clamp loader complex via its δ subunit (21); the other four *E. coli* Pols (Pol I, Pol II, Pol IV, and Pol V) (22–26); the mismatch repair proteins MutS and MutL (22, 27); Hda protein, which together with the β clamp acts to manage the activity of the DnaA replication initiator protein via a process termed regulatory onactivation of DnaA (RIDA [28]); DNA ligase (22); the UmuD protein, which together with UmuC (catalytic subunit of Pol V) is proposed to act as a primitive cell cycle checkpoint control (25, 29); and the chromosomal positioning protein CrfC (30). Of these partners, only the DnaX clamp loader, Pol III replicase, DNA ligase, and Hda are required for *E. coli* viability. While the functional significance of the interactions involving the DnaX clamp loader, Pol III replicase, and Hda are well documented, the importance of the β clamp-DNA ligase interaction is unknown.

The β clamp presumably acts to manage the actions of a variety of proteins involved in DNA metabolism. The Zyskind lab demonstrated that expression of the β clamp at levels $\geq$10-fold higher than chromosomally expressed levels impedes *E. coli* growth by interfering with DNA replication (31). Exploiting this phenotype, we used a multicopy plasmid to elevate the cellular level of the β clamp to select missense mutations in *dnaN* that are not toxic (32, 33). The mutations substitute amino acids distributed throughout the structure of the β clamp protein (Fig. 1). One mutation encoding a V170M substitution resides within the clamp's hydrophobic cleft that is contacted by a consensus clamp binding motif (CBM) located within most, if not all, known clamp partner proteins (26, 34). Another mutation (P363S) is immediately adjacent to the cleft and is required for the interaction with Pol III (35). These findings support the idea that elevated levels of the mutant clamps are unable to interact with Pol III and hence fail to sequester Pol III away from the replication fork. Our results support the model that sequestration of Pol III contributes to growth inhibition and further indicate the existence of at least one additional mechanism that contributes to this phenotype. Importantly, our findings also suggest strongly that physical and functional interactions of the β clamp with Pol III are more extensive than illustrated currently by the available structural information (36).

RESULTS

Locations of the mutations relative to the cryo-electron microscopy (cryo-EM) structure of the β clamp-Pol IIIα-Pol IIIε-DnaXτ_c complex assembled on primed DNA. The interaction of the β clamp with the Pol III holoenzyme, which involves both the Pol III core complex (Pol III$\alpha\varepsilon\theta$) and the DnaX complex through its δ subunit, is

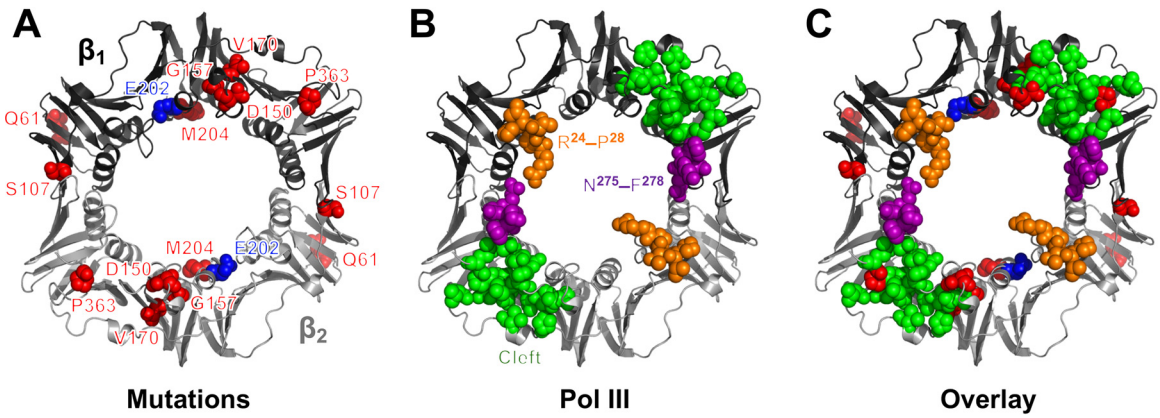

FIG 1 Summary of the positions of β clamp mutations. (A) The positions of the 8 amino acid substitutions analyzed in this work are represented on the X-ray crystal structure of the β clamp (PDB: 1MMI). (B) Positions of clamp surfaces known to interact with Pol III, including the hydrophobic cleft that interacts with the clamp binding motif (CBM) found in many if not all clamp partner proteins (green), and residues ^{24}RPTLP^{28} (orange) and ^{275}NEKF^{278} (purple), which are located within respective solvent exposed loops of the clamp and interact with Pol IIIα only when it is assembled on primed DNA (36). (C) The positions of the 8 amino acid substitutions from panel A superimposed on panel B, illustrating their proximity to clamp surfaces known to contact Pol III. These images were generated using PyMOL v2.4.0.

essential for DNA replication and *E. coli* viability. We hypothesized that the toxicity caused by elevated β clamp levels may be due to the sequestration of one or more of these Pol III subassemblies, rendering them unavailable to support DNA replication in an efficient and processive manner. A prediction is that mutant proteins that are unable to interact with the Pol III core and/or the DnaX clamp loader complex will fail to sequester Pol III away from the replication fork, permitting *E. coli* viability. In support of this idea, the V170M substitution maps to the cleft region of the β clamp in the X-ray structure of the β clamp-δ subunit complex. Likewise, the P363S substitution near the C terminus maps next to the cleft and apparently impedes the interaction of the respective clamp binding motifs in Pol IIIα and Pol IIIε with the hydrophobic cleft of each clamp protomer (Fig. 1) (19, 20, 26, 37–39). These observations provide a mechanistic explanation at the molecular level for the behavior of the mutant V170M and P363S proteins *in vivo*. In contrast, the other mutations do not map to the cleft region.

Recognizing that the structure of the β clamp-δ complex is based on both a mutant clamp ($\beta^{I272A,\ L273A}$) that is unable to homo-dimerize and a truncated form of δ bearing only the N-terminal 140 residues ($\delta^{1\text{-}140}$) (34), our concern was that this structure may not represent the wild-type complex (Fig. 2A). Hence, we instead built a model with the full-length proteins using the structure of the dimeric clamp on DNA (1), as well as that of the full-length δ protein (34). As summarized in Fig. 2B, this model also failed to implicate additional residues beyond those suggested by the crystal structure.

We also considered the positions of the β clamp substitutions in the cryo-EM structure of Pol III (Fig. 2C). Except for V170M and P363S, none of the other β clamp substitutions map to sites that would be expected to impair the interaction of the β clamp with Pol III. While most of the substituted residues are surface exposed in the structure of the unbound β clamp, the G157S substitution is not. Thus, this mutation may affect the local structure of the β clamp. Taken together, these findings suggest either that the wild-type residues represent contacts that are important for β clamp function, which were not captured in the cryo-EM or X-ray crystallographic structures, or that the substitutions alter the 3-dimensional structure of the clamp to interfere with its activity.

Because the cryo-EM and X-ray structures lack the θ subunit of the Pol III core, as well as residues Ala^{928}-Asp^{1160} of Pol IIIα (36), we built an *in silico* model of the Pol III$\alpha\varepsilon\theta$ complex in association with β clamp on DNA. Using full-length proteins, we

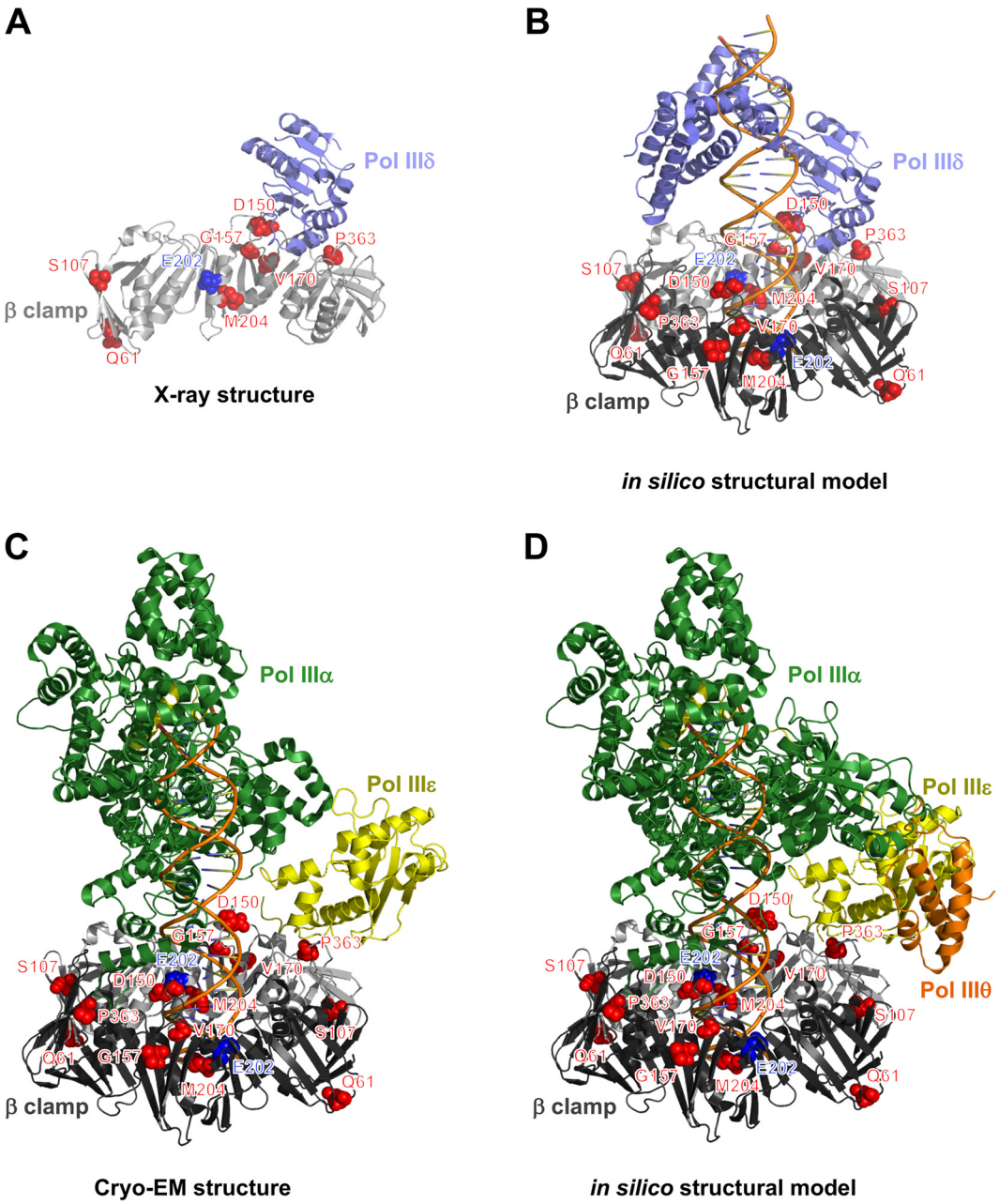

FIG 2 Structural models of the Pol III-β clamp and δ-β clamp complexes showing the positions of β clamp mutations. The positions of the β clamp mutations analyzed in this work are represented on the X-ray crystal structure of the $\delta^{1\text{-}140}$-$\beta^{I272A,\ L273A}$ (β monomer) complex (PDB: 1JQL) (A), the model of the full-length δ-β dimer clamp complex assembled on DNA (B), the cryo-EM structure of the β clamp-Pol IIIα-Pol IIIε-DnaXτ_c assembled on primed DNA (PDB: 5FKW) (C), and the model of the Pol III core-β clamp complex assembled on primed DNA (D). Models presented in panels B and D were constructed as described in the Materials and Methods. The protomers of the β clamp homodimer are shown in dark gray and black, Pol IIIα is green, Pol IIIε is yellow, Pol IIIθ is orange, and Pol IIIδ is purple. DnaXτ_c is not shown, as it does not contact the β clamp exactly as that highlighted above. Positions of amino acid substitutions analyzed in this work are highlighted in red, except for E202, which is in blue. These images were generated using PyMOL v2.4.0.

sought to provide a more complete structural representation for evaluating the impact of additional mutations in the β clamp. The model failed to identify other possible contacts between the clamp and the Pol III core complex (Fig. 2D). However, we note that the substitutions may perturb the transient contacts formed during the dynamic conformational changes borne by the β clamp and Pol III core, which is a major shortcoming of the modeled structure.

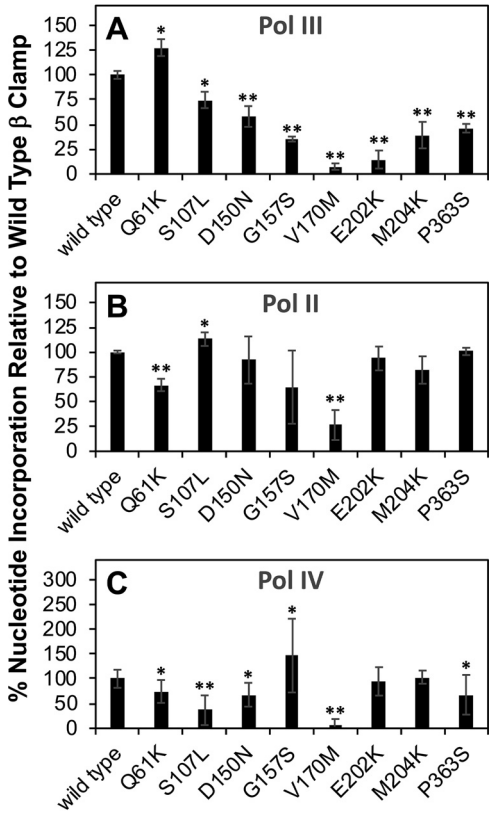

FIG 3 The mutant β clamps are impaired in supporting DNA replication. The ability of the respective mutant β clamp proteins to stimulate replication by Pol III (1 nM for 60 s) (A), Pol II (1 nM for 5 min) (B), or Pol IV (10 nM for 5 min) (C) was measured using an *in vitro* primer extension assay. Results represent the average of 6 determinations ± SD. Levels of nucleotide incorporation (pmol) in the presence of the wild-type β clamp (set equal to 100%) were as follows: 12.9 ± 0.5 for Pol III, 8.7 ± 0.1 for Pol II, and 4.6 ± 0.8 for Pol IV. *, $P \leq 0.05$; **, $P \leq 0.001$; comparisons are relative to the wild-type β control (Student's *t* test).

Activity of the β clamp mutants in primer extension assays. Driven by our interest to understand the biochemical defects of the mutants, which may give added insight into β clamp function, we examined the mutants using several functional assays. We first measured the Pol III-dependent extension of a primer annealed to M13 ssDNA. Considering the locations of the V170M and P363S substitutions, their impaired activity both served to confirm our expectations and acted as a control of sorts. With the exception of β^{Q61K}, which was ~25% more active than the wild-type clamp, all mutants were impaired to various degrees, with β^{V170M} and β^{E202K} having the most severe defects (Fig. 3A).

Because the primer extension assay requires clamp loading by the DnaX clamp loader complex, defective loading instead of problems with binding to Pol III may explain the reduced activity of the mutants with Pol III. Furthermore, our earlier studies suggest strongly that β clamp interactions with Pol III, Pol II, and Pol IV are dissimilar despite the involvement of their respective CBMs (40–42). Thus, we replaced Pol III with either Pol II (Fig. 3B) or Pol IV (Fig. 3C). We found that β^{V170M} was severely impaired in supporting DNA synthesis with all three Pols. As mentioned above, Val-170 is located within the cleft region of the β clamp with which DnaX must interact in order to load the clamp onto DNA (Fig. 1). Thus, β^{V170M} is likely impaired in clamp loading, as well as in its interaction with the different Pols. For the other mutants, β^{Q61K} was modestly defective in supporting Pol II function, whereas β^{S107L} was slightly more proficient than wild-type β. In contrast, β^{Q61K}, β^{S107L}, β^{D150N}, and β^{P363S} were partially impaired for supporting replication by Pol IV, while β^{G157S} was more proficient. The

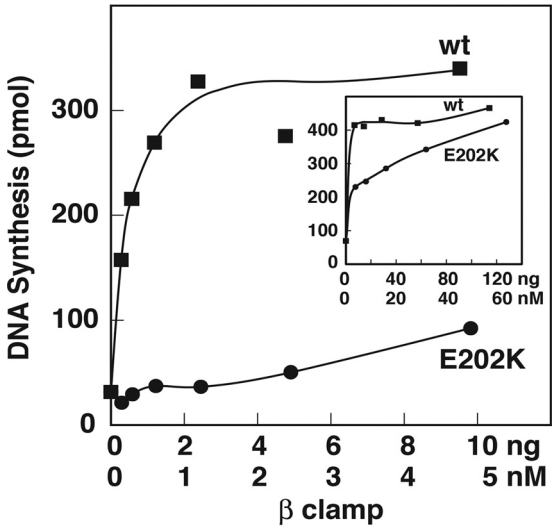

FIG 4 The β^{E202K} clamp is impaired in supporting replication from *oriC in vitro*. The *in vitro* activity of the wild-type β clamp was compared with the β^{E202K} clamp at a range of low and high concentrations (inset).

remaining mutants, including β^{E202K}, supported a level of Pol II and Pol IV replication that was comparable with the wild-type β clamp. The ability of each of the mutant clamps other than β^{V170M} to stimulate DNA replication by at least one of the three Pols suggests that they are able to interact *in vitro* with the DnaX complex and to be loaded onto DNA. Thus, compared with β^{V170M}, these results suggest the other mutant clamps are loaded onto DNA *in vitro* and are instead altered in their interactions with the different Pols.

β^{E202K} is altered in its interaction with the Pol III core. We selected the β^{E202K} mutant for further study for two reasons. First, we had reservations about the biological relevance of the primer extension assay, which suggests that a *dnaN*^{E202K} mutant should be inviable; yet, *in vivo* experiments presented below indicate the opposite. Second, residue E202 of the β clamp failed to contact either the δ subunit of DnaX or Pol III core in either the published structures or our *in silico* models (Fig. 2). To address the first issue, we measured the activity of β^{E202K} in DNA replication of an *oriC*-containing plasmid. This *in vitro* system appears to recapitulate replication initiation *in vivo*, which involves the DnaA-mediated assembly of dimeric replisomes for the concerted synthesis of each leading and lagging DNA strand under a mode of bidirectional fork movement (43). Using this assay, the wild-type β clamp supported a robust level of Pol III-dependent replication from *oriC* at levels as low as 0.5 nM (Fig. 4). In contrast, the activity of β^{E202K} was impaired substantially, requiring $>$10-fold higher levels to support a similar level of activity as the wild-type clamp (inset of Fig. 4).

Turning to the issue of whether the E202K substitution in the β clamp affects its interaction with Pol III core, the DnaX complex, or both, we measured the ability of β^{E202K} to bind to these partners using surface plasmon resonance (SPR). We first analyzed the interaction of the β clamp with the δ subunit of DnaX, which is the primary point of contact between the DnaX complex and the β clamp (34). We demonstrated previously that the mutant β^{C} clamp, which lacks the cleft region, failed to interact with δ by SPR (see the footnotes to Table 1) (44), confirming that this interaction requires the clamp cleft. We further showed that a single β clamp can interact with two δ protomers in which the binding of the first protomer to the cleft of one clamp subunit has a negatively cooperative effect with the binding of the second protomer to the cleft of the other clamp subunit (44). We therefore used a two-site model for the analysis of the SPR data. The results summarized in Table 1 indicate that the wild-type

TABLE 1 Interaction of the wild-type β and β^{E202K} clamp with the δ subunit of the DnaX clamp loader complex and Pol III$\alpha\varepsilon\theta$ catalytic core complex[a]

					Avg[c] (range) of:	
Interaction[b]	Expt	K_D (nM)	k_a ($M^{-1}s^{-1}$)	k_d (s^{-1})	K_{D1} (nM)	K_{D2} (nM)
$^{His}\beta$-δ	1	K_{D1} = 93.8	1.54×10^3	1.45×10^{-4}	88.0 (11.7)	314 (39.7)
		K_{D2} = 294	3.50×10^4	1.03×10^{-2}		
	2	K_{D1} = 82.1	5.20×10^3	4.27×10^{-4}		
		K_{D2} = 334	3.54×10^4	1.18×10^{-2}		
$^{His}\beta^{E202K}$-δ	1	K_{D1} = 150	3.26×10^4	4.89×10^{-3}	148 (3.67)	182 (45.6)
		K_{D2} = 204	1.29×10^3	2.64×10^{-4}		
	2	K_{D1} = 146	3.53×10^4	5.17×10^{-3}		
		K_{D2} = 159	1.31×10^3	2.08×10^{-4}		
Pol III$\alpha\varepsilon\theta^{His}$-$\beta$	1	K_{D1} = 19.2	2.68×10^4	5.15×10^{-4}	15.3 (7.67)	56.7 (22.2)
		K_{D2} = 45.6	3.64×10^5	1.66×10^{-2}		
	2	K_{D1} = 11.5	2.80×10^4	3.22×10^{-4}		
		K_{D2} = 67.8	2.56×10^5	1.66×10^{-2}		
Pol III$\alpha\varepsilon\theta^{His}$-$\beta^{E202K}$	1	K_{D1} = 1.92	6.38×10^4	1.23×10^{-4}	2.20 (0.56)	205 (3.70)
		K_{D2} = 203	8.01×10^4	1.63×10^{-2}		
	2	K_{D1} = 2.48	3.50×10^4	8.69×10^{-5}		
		K_{D2} = 207	8.62×10^4	1.78×10^{-2}		

[a]We demonstrated previously that an interaction of $^{His}\beta^{C}$ with δ was not detected by SPR (44); $^{His}\beta^{C}$ lacks its C-terminal five residues, which disrupts the hydrophobic cleft to which the δ clamp binding motif associates (44).
[b]The indicated N-terminally His_6-tagged protein (β^{His}, $^{His}\beta^{E202K}$, or Pol III$\alpha\varepsilon\theta^{His}$) was attached to the SPR sensor surface using penta-His antibody (Qiagen). The indicated untagged analyte (δ, β, or β^{E202K}) was then flowed over the sensor surface. Interactions were analyzed using the two-site binding model. Instead of χ^2 (goodness of fit), the ClampXP 3.50 software provides residual sum of squares (goodness of fit), which were each <10% of the respective R_{max}, confirming the specificity of each interaction.
[c]From 2 independent experiments.

and β^{E202K} clamps display affinities for δ that were within 2-fold of each other. This finding is consistent with the primer extension experiments wherein β^{E202K} was proficient for stimulating replication by Pol II and Pol IV, indicating that β^{E202K} was loaded onto DNA *in vitro* by DnaX (Fig. 3B and C). Despite the similar affinities of β^{E202K} and the wild-type clamp for δ, the mutant displayed higher on and off rates for K_{D1} but lower on and off rates for K_{D2}. Taken together, these results support the conclusion that the major defect of the β^{E202K} clamp is not at the level of clamp loading.

We next analyzed the Pol III complex (Pol III$\alpha\varepsilon\theta$). Because the Pol IIIα catalytic and the Pol IIIε proofreading subunits each bind to separate hydrophobic clefts of a β clamp dimer (19, 20, 36) (Fig. 2C and D), we used a two-site model to analyze their interactions. As summarized in Table 1, the first site in the Pol III core complex (Pol III$\alpha\varepsilon\theta$) interacted ~7-fold more strongly with the β^{E202K} clamp compared with the wild-type clamp, while its second site exhibited an ~4-fold weaker interaction. Specifically, the Pol III core bound the wild-type β clamp with equilibrium dissociation constant (K_D) values of 15.3 ± 7.67 nM (K_{D1}) and 56.7 ± 22.2 nM (K_{D2}), while it bound the β^{E202K} clamp with K_D values of 2.20 ± 0.56 nM (K_{D1}) and 204.8 ± 3.70 nM (K_{D2}).

We next analyzed the interaction of the β clamp with Pol IIIα and Pol III$\varepsilon\theta$ using biolayer interferometry (BLI). Since (i) we determined previously that the β clamp contacts sites on Pol IIIα in addition to its cleft (44) and (ii) the BLI data did not fit well to the 1:1 interaction model (χ^2 = 1.812 and R^2 = 0.934 versus χ^2 = 2.779 and R^2 = 0.943 for the wild-type and β^{E202K} clamps, respectively), we used the heterogeneous 1:2 site model. As summarized in Table 2, results for both wild-type β and β^{E202K} fit well to the heterogenous model and displayed similar K_{D1} values (251 and 209 nM, respectively). However, the K_{D2} for the wild-type clamp was almost 3-fold higher than the K_{D2} for β^{E202K} (308 and 114 nM, respectively), indicating that β^{E202K} has a modestly higher affinity for Pol IIIα. As a negative control, we measured the interaction of Pol IIIα with the

TABLE 2 Interaction of the wild-type and β^{E202K} clamp with Pol IIIα

Interaction[a]	Expt	K_D (nM)	k_a ($M^{-1}s^{-1}$)	k_d (s^{-1})	Avg[b] (range) of: K_{D1} (nM)	Avg[b] (range) of: K_{D2} (nM)
Pol IIIα^{His}-β^{C}	1, 2	ND[c]	NA[c]	NA	ND	ND
Pol IIIα^{His}-β^{+}	1	K_{D1} = 228	1.79×10^4	4.09×10^{-3}	251 (45.0)	308 (90.0)
		K_{D2} = 263	1.97×10^6	5.17×10^{-1}		
	2	K_{D1} = 273	1.57×10^4	4.29×10^{-3}		
		K_{D2} = 353	1.41×10^6	4.99×10^{-1}		
Pol IIIα^{His}-β^{E202K}	1	K_{D1} = 221	2.25×10^4	4.96×10^{-3}	209 (24.0)	114 (28.9)
		K_{D2} = 128	2.56×10^6	3.26×10^{-1}		
	2	K_{D1} = 197	2.48×10^4	4.89×10^{-3}		
		K_{D2} = 99.1	3.47×10^6	3.44×10^{-1}		

[a]Interaction of Pol IIIα^{His} (ligand) with untagged β^{C}, β^{+}, or β^{E202K} (analyte) was measured using an Octet RED 96e BLI instrument (Sartorius) equipped with penta-His (HIS1K) Dip and Read biosensor tips. χ^2 values (likelihood of no relationship) ranged from 0.053 to 0.108, while R^2 (goodness of fit) was 0.998 for each fit to the heterogeneous 1:2 site interaction model.
[b]Results represent the average from 2 independent experiments.
[c]ND, none detected; NA, not applicable.

mutant β^{C}. We failed to detect an interaction by BLI (Table 2), which confirms earlier findings that Pol IIIα binds to the clamp's cleft region (26, 36). For additional controls, we measured the interaction of β^{E202K} with Pol II and Pol IV. β^{E202K} was comparable with the wild-type clamp for stimulating the replication activity of these Pols *in vitro* (Fig. 3B and C). Consistent with this finding, the respective affinities of the wild-type and β^{E202K} clamp proteins for Pol II and Pol IV were each within 2-fold of each other, and respective on rates (k_a) and off rates (k_d) were also similar (Table 3). Efforts to analyze the β clamp-Pol III$\varepsilon\theta$ interaction yielded variable results in the low- to mid-micromolar range, suggesting that this interaction is too weak to be reliably measured by BLI. Nevertheless, the results that β^{E202K} has a higher affinity for Pol IIIα, as well as both higher and lower affinities with sites in the Pol III core, presumably explain its impaired

TABLE 3 Interaction of the wild-type β and β^{E202K} clamp with Pol II and Pol IV

Interaction[a]	Expt	K_D (nM)	k_a ($M^{-1}s^{-1}$)	k_d (s^{-1})	Avg[b] (range) of: K_{D1} (nM)	Avg[b] (range) of: K_{D2} (nM)
Pol II^{His}-β^{+}	1	K_{D1} = 309	7.62×10^3	2.36×10^{-3}	362 (105)	58.7 (29.3)
		K_{D2} = 73.3	9.70×10^5	7.11×10^{-2}		
	2	K_{D1} = 414	6.58×10^3	2.72×10^{-3}		
		K_{D2} = 44.0	1.88×10^6	8.27×10^{-2}		
Pol II^{His}-β^{E202K}	1	K_{D1} = 642	6.08×10^3	3.91×10^{-3}	598 (88.0)	83.9 (14.3)
		K_{D2} = 91.0	8.65×10^5	7.87×10^{-2}		
	2	K_{D1} = 554	6.83×10^3	3.79×10^{-3}		
		K_{D2} = 76.7	1.17×10^6	9.00×10^{-2}		
Pol IV^{His}-β^{+}	1	K_{D1} = 23.2	5.09×10^4	1.18×10^{-3}	21.0 (4.50)	26.0 (0.40)
		K_{D2} = 26.2	1.11×10^6	2.92×10^{-2}		
	2	K_{D1} = 18.7	5.31×10^4	9.89×10^{-4}		
		K_{D2} = 25.8	1.16×10^6	2.99×10^{-2}		
Pol IV^{His}-β^{E202K}	1	K_{D1} = 44.1	2.53×10^4	1.12×10^{-3}	40.5 (7.30)	37.9 (1.10)
		K_{D2} = 37.3	8.56×10^5	3.19×10^{-2}		
	2	K_{D1} = 36.8	2.53×10^4	9.31×10^{-4}		
		K_{D2} = 38.4	8.32×10^5	3.19×10^{-2}		

[a]Interaction of the indicated His_6-tagged Pol (ligand) with untagged β^{+} or β^{E202K} (analyte) was measured using an Octet RED 96e BLI instrument (Sartorius) equipped with penta-His (HIS1K) Dip and Read biosensors. χ^2 values (likelihood of no relationship) ranged from 0.041 to 1.873, while R^2 (goodness of fit) ranged from 0.991 to 0.997 for each fit to the heterogeneous 1:2 site interaction model.
[b]Results represent the average from 2 independent experiments.

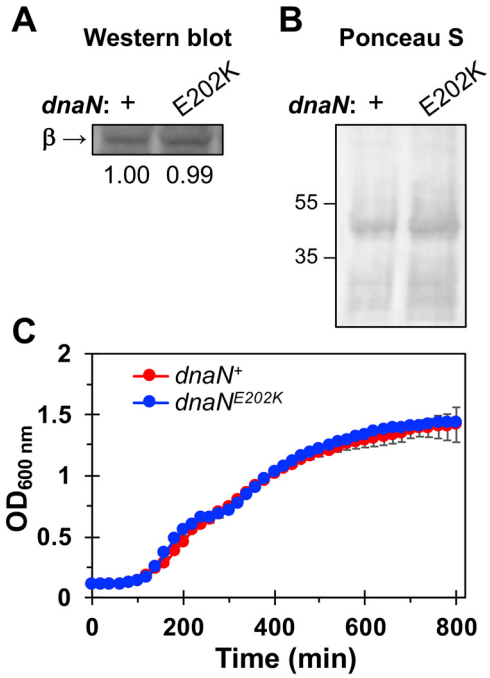

FIG 5 Cellular levels of the mutant β^{E202K} clamp and growth of the *dnaN*^{E202K} strain. (A) The relative β clamp levels in isogenic *dnaN*$^{+}$ (*E. coli* VB001) and *dnaN*^{E202K} (*E. coli* VB019) strains were measured in whole-cell lysates by quantitative Western blot analysis. Results represent the average from triplicate analyses. (B) Ponceau S-stained PVDF membrane following transfer but prior to Western blot analysis was performed to confirm the uniformity of protein transfer. (C) The growth of isogenic *dnaN*$^{+}$ and *dnaN*^{E202K} strains at 37°C in LB medium with aeration was monitored as a function of time by measuring optical density at 600 nm (OD_{600}). Results represent the average of triplicates ± SD.

ability to stimulate Pol III replication *in vitro* (Fig. 3A and 4). We suggest that the altered affinities of β^{E202K} for Pol III perturb one or more conformational changes required for proper Pol III HE function.

The *dnaN*^{E202K} allele supports *E. coli* viability but modestly induces the global SOS response to DNA damage. The impaired *in vitro* activity of the mutant β^{E202K} clamp protein with respect to stimulating Pol III replication suggests that a strain carrying the defective protein in place of the wild-type β clamp may fail to grow or display reduced growth. We determined previously that the *dnaN*^{E202K} allele supports *E. coli* viability when expressed from a low copy number plasmid using a plasmid shuffle assay (32). To determine if the chromosomally expressed level of the β^{E202K} mutant clamp supports *E. coli* viability, we used λ-recombineering to replace the *dnaN*$^{+}$ allele with *dnaN*^{E202K} in strain MG1655. Quantitative Western blot experiments showed that the steady-state level of the mutant β^{E202K} clamp was comparable with that of the wild-type protein (Fig. 5A and B), suggesting that the E202K substitution does not alter the stability of the mutant protein. Hence, the indistinguishable growth rates of the isogenic *dnaN*$^{+}$ and *dnaN*^{E202K} strains (Fig. 5C) suggest that the *dnaN*^{E202K} allele supports essential clamp functions *in vivo*.

The comparable growth rates of the isogenic *dnaN*^{E202K} and *dnaN*$^{+}$ strains (Fig. 5C) contrast with the biochemical defect of the mutant protein in Pol III-dependent DNA synthesis *in vitro* (Fig. 3A and 4). Because the measurement of growth rate does not necessarily reflect difficulties in replicating the bacterial genome, which would lead to increased levels of single-stranded DNA that results in the induction of the global SOS response (45), we considered if the *dnaN*^{E202K} allele caused this pathway to be induced. The SOS response comprises a regulon of more than 50 unlinked genes, and its induction acts to pause the cell cycle, elevate DNA repair, and activate DNA damage tolerance by translesion DNA synthesis (TLS) (reviewed in reference 4). To assess the induction of the SOS response, we used quantitative PCR (qPCR) to measure *lexA* and *sulA*

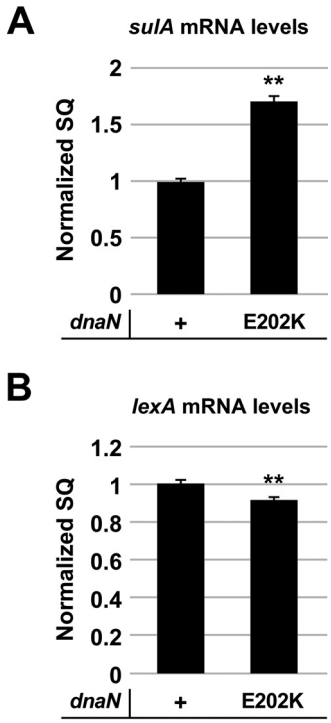

FIG 6 Quantitation of *sulA* and *lexA* transcript levels. The levels of *sulA* (A) and *lexA* (B) transcripts in isogenic *dnaN*$^{+}$ (*E. coli* VB001) and *dnaN*^{E202K} (*E. coli* VB019) strains were measured by qPCR, and values were normalized relative to *hcaT* mRNA. The average of 3 determinations ± SD is shown. **, $P \leq 0.001$; relative to the *dnaN*$^{+}$ control (Student's *t* test).

transcript levels. LexA regulates SOS response genes that include *sulA*, which controls cell division by inhibiting FtsZ-dependent septum formation required for cell division (46, 47). As shown in Fig. 6, the *lexA* levels were decreased modestly, but *sulA* levels were ~1.6-fold higher in the *dnaN*^{E202K} mutant relative to the *dnaN*$^{+}$ control. The higher level of *sulA* expression is consistent with a modest induction of the SOS response.

Given that *lexA* levels were changed marginally while *sulA* levels were increased (Fig. 6), we isolated fresh RNA and used transcriptome sequencing (RNA-seq) to compare the steady-state transcript levels of the 55 known SOS-regulated genes in both the *dnaN*$^{+}$ and *dnaN*^{E202K} strains. Examination of the SOS genes indicated that 12 were expressed at levels that varied by ≥50% compared with the *dnaN*$^{+}$ control (Table 4). Levels for 7 of these 12 genes were increased by ≥50% compared with those of *dnaN*$^{+}$, while the remaining 5 were reduced by ≥50%. Consistent with our qPCR results, *sulA* levels were elevated by ~50%, while *lexA* levels were reduced by ~6%. Transcription of 3 (*ibpA*, *ibpB*, and *ydeO*) of the 5 SOS-regulated genes whose expression was reduced in the *dnaN*^{E202K} mutant strain is regulated by at least 8 transcription factors in addition to LexA (48, 49). Thus, the reduced levels of these transcripts may be unrelated to SOS. Taken together, the results discussed above support the view that SOS is induced modestly in the *dnaN*^{E202K} strain.

To gain insight into whether the *dnaN*^{E202K}-encoded mutant clamp impaired genome replication *in vivo*, we compared this mutant to the isogenic *dnaN*$^{+}$ strain by flow cytometry. Under the conditions of replication runout, the treatment of log-phase cultures with rifampicin and cephalexin inhibits new rounds of chromosomal DNA replication and cell division, respectively, but permits ongoing replication forks to complete synthesis (50, 51). Cells that initiate synchronously carry 2^N chromosomes where N is an integer equal to or larger than 0. Flow cytometry revealed cells with two and four chromosomes for both strains, as well as a small population of wild-type cells

TABLE 4 Expression levels of SOS-regulated genes in the *dnaN*^{E202K} strain

Gene	Gene ID[a]	Gene function[b]	Fold change in expression level relative to *dnaN*$^{+}$ control[c]
lexA	b4043	Transcriptional repressor of SOS regulon	−1.06
recA	b2699	Recombinase involved in SOS induction	+1.17
recN	b2616	Recombination	+1.06
ruvA	b1861	Holiday junction branch migration	+1.12
ruvB	b1860	Holiday junction branch migration	+1.25
dinI	b1061	Stabilizes RecA-single-strand DNA filaments	+1.22
rmuC	b3832	Putative recombination limiting protein	−1.19
sulA	b0958	Inhibitor of cell division	+1.46
ftsK	b0890	Chromosome segregation	+1.08
insK	b3558	IS*150* conserved protein	+1.31
intE	b1140	Predicted e14 prophase integrase	+1.06
lit	b1139	e14 prophage cell death peptidase involved in phage exclusion	+1.52
ogrK	b2082	Phage P2 late control protein	+1.25
borD	b0557	Prophage DLP12 lipoprotein	+1.06
grxA	b0849	Glutoredoxin	−1.03
sbmC	b2009	DNA gyrase inhibitor	+1.18
ssb	b4059	Single-stranded DNA binding protein	+1.19
uvrA	b4058	Nucleotide excision repair	+1.07
uvrB	b0779	Nucleotide excision repair	+1.48
uvrD	b3813	Nucleotide excision repair	−1.14
cho	b1741	Nucleotide excision repair	+1.02
dinG	b0799	ATP-dependent DNA helicase	+1.28
yoaA	b1808	DinG-family helicase	+1.14
polB	b0060	Pol II, replication, TLS	+1.14
dinB	b0231	Pol IV (DinB), TLS	+1.02
umuD	b1183	$UmuD_2C$ DNA damage checkpoint control, Pol V ($UmuD'_2C$), TLS	+1.25
umuC	b1184	$UmuD_2C$ DNA damage checkpoint control, Pol V ($UmuD'_2C$), TLS	−1.09
ibpA	b3687	Heat-inducible chaperone protein complex	−1.96
ibpB	b3686	Heat-inducible chaperone protein complex	−1.82
ydeO	b1499	AraC/XylS family of transcriptional regulators	−3.86
hokE	b4415	Toxin protein	+1.58
dinQ	b4613	Toxin protein	1.00
tisB	b4618	Toxic peptide	1.00
symE	b4347	Toxin-like protein	−1.30
dinF	b4044	Multiantimicrobial extrusion transporter	−1.91
ydjM	b1728	Inner membrane protein	+1.62
yccF	b0961	Inner membrane protein	+1.63
yifL	b4558	Predicted lipoprotein	−1.40
rlmF	b0807	Ribosomal RNA large subunit methyltransferase F	+1.91
ydeR	b1503	Predicted fimbrial protein	+1.29
ydeS	b1504	Predicted fimbrial protein	−1.17
ydeT	b1505	Fimbrial usher protein	−2.09
arpB	b4494	*orf* with unknown function	+2.21
pcsA	b3645	*orf* with unknown function	−1.10
ybfE	b0685	*orf* with unknown function	+1.60
ycgH	b4491	*orf* with unknown function	+1.27
yebG	b1848	*orf* with unknown function	+1.31
yhiJ	b3488	*orf* with unknown function	−1.32
yoaB	b1809	*orf* with unknown function	+1.20
yqgC	b2940	*orf* with unknown function	+1.33
ymfD	b1137	e14 prophage *orf* with unknown function	–1.39
ymfE	b1138	e14 prophage *orf* with unknown function	–1.20
ymfG	b1141	e14 prophage *orf* with unknown function	+1.01
ymfI	b1143	e14 prophage *orf* with unknown function	−1.06
ymfJ	b1144	e14 prophage *orf* with unknown function	−1.07

[a]ID, identifier.
[b]Gene function was defined by EcoCyc (https://ecocyc.org).
[c]A negative sign indicates a fold reduction in the transcript level relative to the isogenic *dnaN*$^{+}$ control, whereas a positive sign indicates a fold increase.

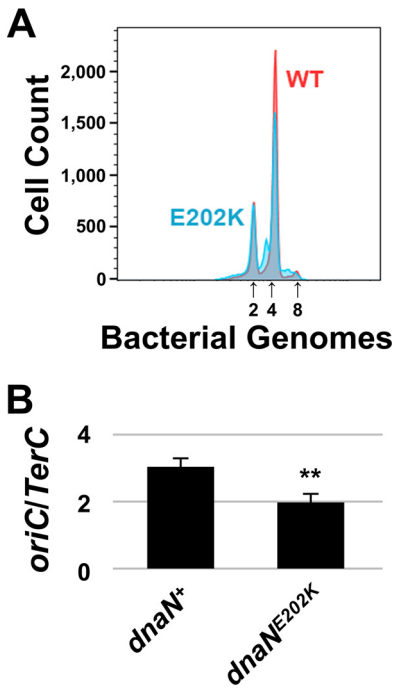

FIG 7 Genome content of the *dnaN*^{E202K} mutant. (A) Genome content of isogenic *dnaN*$^{+}$ and *dnaN*^{E202K} strains was measured by flow cytometry following replication run-out. Results are representative of 2 independent experiments. (B) *oriC*/*TerC* ratios of isogenic *dnaN*$^{+}$ and *dnaN*^{E202K} strains were measured using qPCR and represent the average of 3 determinations ± SD. **, $P \leq 0.001$; relative to the *dnaN*$^{+}$ control (Student's *t* test).

containing eight chromosomes. In addition, a small shoulder on both sides of the four-chromosome peak was observed in *dnaN*^{E202K} mutant cells (Fig. 7A). This subpopulation has a non-2N DNA content. The non-2N content in the *dnaN*^{E202K} strain suggests a failure to complete replication, consistent with our *in vitro* results demonstrating that β^{E202K} is impaired in supporting Pol III replication function (Fig. 3A and 4). The lack of *dnaN*^{E202K} cells bearing eight chromosomes and the slightly higher relative proportion of *dnaN*^{E202K} cells with two chromosomes compared with four chromosomes suggests less frequent initiation compared with the *dnaN*$^{+}$ strain. Consistent with this finding, the *dnaN*^{E202K} strain contained a reduced *oriC*/*Ter* ratio as measured by qPCR (Fig. 7B). Finally, we failed to observe significant cell elongation in the *dnaN*^{E202K} strain, as indicated by the small fraction of cells with a higher genome content at the right of the peak corresponding with four genome equivalents in flow cytometry (Fig. 7A) (52), consistent with SOS induction in only a subpopulation of *dnaN*^{E202K} cells. If cell elongation were considerable, this subpopulation would be more substantial.

The *dnaN*^{E202K} strain is proficient in DNA damage-induced mutagenesis but is nevertheless sensitive to UV light (UV) and MMS. In light of the results discussed above suggesting that the mutant β^{E202K} clamp is impaired in supporting Pol III replication (Fig. 3A, 4, 6, and 7, Table 4), we hypothesized that the *dnaN*^{E202K} mutant displays an enhanced level of sensitivity to DNA damage compared with the isogenic *dnaN*$^{+}$ strain. To test this hypothesis, we measured the sensitivity of the *dnaN*$^{+}$ and *dnaN*^{E202K} strains to methyl methanesulfonate (MMS) and UV light. Pol IV is able to replicate over alkyated bases generated by MMS (53), whereas Pol V bypasses abasic sites generated by MMS, as well as UV-induced DNA damage (reviewed in reference 4). As shown in Fig. 8, the *dnaN*^{E202K} strain was ~100-fold more sensitive to 5 mM or 6 mM MMS compared than the *dnaN*$^{+}$ control, while the isogenic *dnaN*$^{+}$ Δ*dinB* strain displayed pronounced sensitivity at 3 mM MMS and also higher levels (Fig. 8A). Compared with the *dnaN*$^{+}$ control, the *dnaN*^{E202K} strain was ~10-fold more sensitive to UV (Fig. 8B). These results suggest that β^{E202K} largely supports the function of Pol V *in vivo* but may be

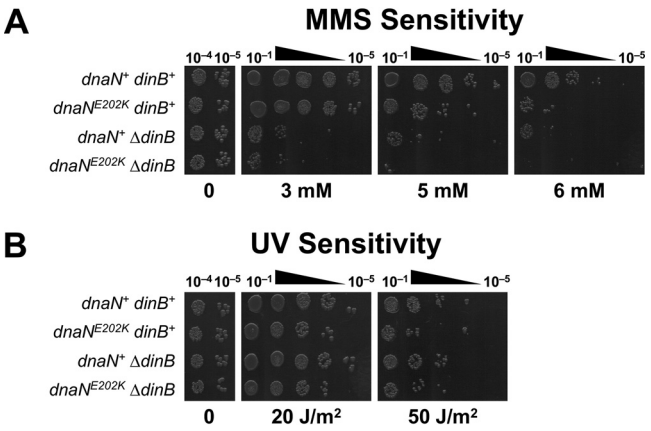

FIG 8 The *dnaN*^{E202K} mutant is marginally sensitized to UV and is severely sensitized to methyl methanesulfonate. Sensitivity of isogenic *dnaN*$^{+}$ (*E. coli* VB001), *dnaN*^{E202K} (*E. coli* VB019), *dnaN*$^{+}$ Δ*dinB* (*E. coli* VB023), and *dnaN*^{E202K} Δ*dinB* (*E. coli* VB024) strains to MMS (A) or UV light (B) was measured as described in the Materials and Methods. Representative results of 3 independent experiments are shown.

impaired in supporting Pol IV, which contrasts with the ability of β^{E202K} to stimulate Pol IV replication *in vitro* (Fig. 3C). However, our finding that the *dnaN*^{E202K} Δ*dinB* strain was more sensitive to MMS than the *dnaN*^{E202K} or Δ*dinB* strains indicates that these two alleles are not epistatic. Thus, the MMS sensitivity observed with the *dnaN*^{E202K} strain does not appear to be the result of the failure of the β^{E202K} clamp to support Pol IV function *in vivo* (Fig. 8A). In contrast, UV sensitivity of the *dnaN*^{E202K} and *dnaN*^{E202K} Δ*dinB* strains was similar (Fig. 8B), consistent with the β^{E202K} clamp supporting Pol V function *in vivo* and Pol IV failing to play a role in bypassing UV photoproducts *in vivo* (reviewed in reference 4).

In addition to cell killing, exposure of *E. coli* to MMS and UV also impacts the mutation frequency in a manner that is dependent on specific TLS Pols (reviewed in reference 4). As summarized in Fig. 9, the frequency of rifampicin resistance (Rif^{r}) for the *dnaN*^{E202K} strain following exposure to MMS or UV was indistinguishable from that of the isogenic *dnaN*$^{+}$ control. These results suggest that the observed MMS and UV sensitivity of the *dnaN*^{E202K} strain is a result of the observed Pol III replication defect (Fig. 3A and 4) and/or one or more as-yet-undefined DNA repair defects.

Viability of the *dnaN*^{E202K} strain is unaffected by elevated levels of the nonessential *E. coli* DNA polymerases. Mutation of the *E. coli* β clamp (42, 54), the Rep helicase (55), or the ψ subunit of the DnaX clamp loader complex (56) interferes with the normal coordination between Pol III and the different accessory Pols (i.e., Pols I, II, IV, and V) during DNA replication, leading to significantly reduced cell viability. In the case of the *dnaN159* strain, the lower affinity of the mutant β159 clamp for each of the five *E. coli* Pols results in their mismanagement *in vivo* and poor viability (40, 42). As the mutant β^{E202K} clamp is altered in its interaction with Pol III as well as its ability to support Pol III replication both *in vitro* (Fig. 3A and 4) and *in vivo* (Table 4 and Fig. 6 and 7), we investigated whether elevated levels of Pol I, Pol II, Pol IV, or Pol V affected growth of the *dnaN*^{E202K} strain using an established quantitative transformation assay. Using this method, we showed previously that elevated levels of Pol I or Pol IV interfered with Pol III replication in *dnaN159* or Δ*rep* strains (54, 55). Briefly, transformation efficiencies of low copy number plasmids directing the elevated expression of Pol I (~3,600 molecules per cell), Pol II (~7,600 molecules per cell), Pol IV (~3,800 molecules per cell), or the activated form of Pol V (~240 UmuD′$_2$C molecules per cell) from their native promoters were measured using as hosts the isogenic *dnaN*$^{+}$ (CH100) and *dnaN*^{E202K} (CH101) strains. The *dnaN159* strain (MS105) was also examined as a control. Because Pol II, Pol IV, and Pol V are SOS regulated, the strains also contained the *lexA51*(Def) mutation to relieve LexA-mediated transcriptional repression of the plasmid-encoded

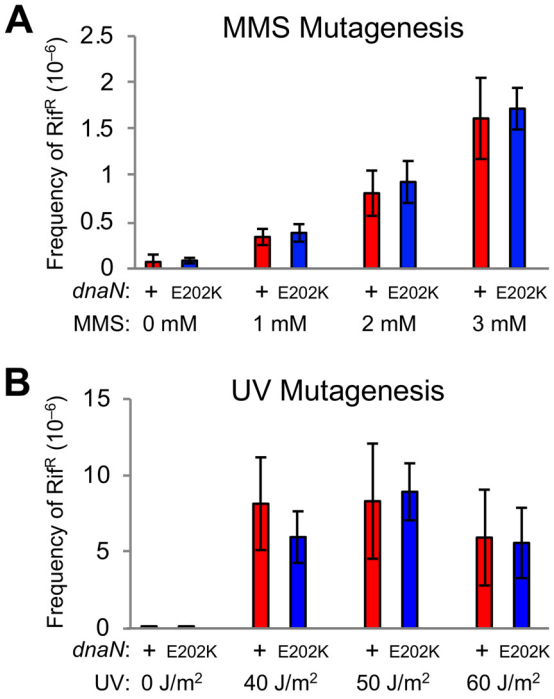

FIG 9 The *dnaN*^{E202K} mutant remains competent in its response to potential mutagens. Frequencies of spontaneous and DNA damage-induced Rif^r of isogenic *dnaN*$^+$ (*E. coli* VB001) and *dnaN*^{E202K} (*E. coli* VB019) strains following mock treatment or treatment with MMS (A) or UV light (B) were measured as described in the Materials and Methods. Values represent the average of 8 determinations ± SD.

TLS Pols. As summarized in Table 5, the transformation efficiencies of the *dnaN*^{E202K} strain observed with each plasmid irrespective of the growth temperature were comparable with that of the control plasmid (pWSK29) that was used to construct the different Pol-expressing plasmids. Although these results are similar to what we observed for the isogenic *dnaN*$^+$ control strain, they contrast with those observed with the *dnaN159* strain, which as observed previously was severely sensitized to both the Pol I- and Pol IV-expressing plasmids (54). These results suggest that the increased affinity of β^{E202K} for Pol III prevents these accessory Pols from inappropriately replacing Pol III at the replication fork *in vivo* despite the reduced ability of β^{E202K} to support Pol III replication *in vitro* (Fig. 3A and 4) and *in vivo* (Table 4 and Fig. 6 and 7).

DISCUSSION

Expression of the *E. coli* β clamp at ≥10-fold higher than chromosomally expressed levels impedes growth by interfering with DNA replication (31). We hypothesized that

TABLE 5 Viability of the *dnaN*^{E202K} strain is affected marginally by elevated steady-state levels of accessory Pols

Transforming plasmid	Transformation efficiency[a] of:				
	dnaN159 lexA51(def)	*dnaN*$^+$ *lexA51*(Def)		*dnaN*^{E202K} *lexA51*(Def)	
	30°C	30°C	37°C	30°C	37°C
pWSK29 (control)	2.3 (±0.7) × 10^3 (≡1.0)	2.5 (±0.8) × 10^3 (≡1.0)	2.7 (±2.1) × 10^3 (≡1.0)	1.9 (±0.1) × 10^3 (≡1.0)	2.7 (±1.4) × 10^3 (≡1.0)
pRM100 (Pol I)	10 (±<0.1) (0.004)	1.5 (±0.1) × 10^3 (0.6)	2.1 (±0.7) × 10^3 (0.8)	1.4 (±0.5) × 10^3 (0.7)	2.9 (±2.7) × 10^3 (1.1)
pRM101 (Pol II)	1.8 (±0.01) × 10^3 (0.8)	1.3 (±1.0) × 10^3 (0.5)	3.5 (±1.8) × 10^3 (1.3)	1.1 (±0.1) × 10^3 (0.6)	6.6 (±5.1) × 10^3 (2.4)
pRM102 (Pol IV)	<6.7 (<0.003)	1.4 (±0.6) × 10^3 (0.6)	3.3 (±2.3) × 10^3 (1.2)	1.8 (±1.4) × 10^3 (1.0)	5.1 (±1.9) × 10^3 (1.9)
pRM103 (Pol V)	1.9 (±1.1) × 10^3 (0.8)	2.0 (±1.8) × 10^3 (0.8)	3.9 (±1.8) × 10^3 (1.5)	1.0 (±0.2) × 10^3 (0.6)	8.6 (±1.9) × 10^3 (3.2)

[a]Transformation efficiencies of strains MS105 (*dnaN159 lexA51*[Def]), CH100 (*dnaN*$^+$ *lexA51*[Def]), and CH101 (*dnaN*^{E202K} *lexA51*[Def]) with the indicated plasmids are the average from two experiments and are expressed as CFU per microgram of DNA ± range. Because the *dnaN159* strain is thermolabile, the transformation efficiency of strain MS105 was measured only at 30°C. Values in parentheses represent the fold change in transformation efficiency relative to the pWSK29 control (that was set equal to 1.0) for each respective strain and temperature.

elevated levels of the clamp are able to sequester Pol III to impair its activity in DNA replication. As a test of this hypothesis, we characterized 8 mutant clamp proteins that were identified by virtue of their inability to impede growth when expressed from a multicopy plasmid (32, 33). For β^{G157S}, β^{V170M}, and β^{P363S}, our results suggest that they are defective in sequestering Pol III. Specifically, these mutant proteins were impaired for stimulation of Pol III replication *in vitro* (Fig. 3A), which correlated with their weakened interactions with Pol IIIα *in vitro* based on gel filtration experiments and the locations of the substitutions for V170M and P363S relative to the X-ray structure and clamp surfaces known to interact with Pol IIIα (Fig. 2) (39). In the case of G157S, which is not surface exposed, the substitution may alter a substructure that may then affect the structural context of other critical residues or interfere with a conformational change required for clamp function.

In an earlier study, we assessed the ability of the remaining mutants to interact with Pol III using a qualitative gel filtration chromatography assay (39). They were at best affected only modestly. In the current work, using a quantitative method that focused on the β^{E202K} clamp, it has a higher affinity for Pol IIIα *in vitro* than the wild-type clamp (Table 1). Based on the cryo-EM structure of the β clamp-Pol IIIα-Pol IIIε-DnaXτ_c complex with and without primed DNA, Pol IIIα is suggested to contact the clamp cleft independently of DNA and in the presence of DNA to additionally contact residues Arg^{24}-Pro^{28} and Asn^{275}-Phe^{278} (Fig. 1) (36). In contrast, details regarding the Pol IIIε-β clamp interaction were not defined clearly in the cryo-EM structure, although prior work demonstrated that Pol IIIε likely binds only the clamp cleft (57). Using our structural model of the β clamp-Pol III$\alpha\varepsilon\theta$-DNA complex (Fig. 2C and D), none of our β clamp mutations, except V170M and P363S that target the CBM-clamp cleft interaction, appear to affect residues that make direct contact with Pol IIIα or Pol IIIε. This poor understanding highlights the limitations of the static structural models lacking important subunits and emphasizes that our knowledge about the function of the β clamp is very incomplete. Taken together, these results suggest that the benign effect of elevated levels of β^{E202K} and possibly β^{Q61K}, β^{S107L}, β^{D150N}, and β^{M204K} on *E. coli* viability is not a result of their inability to interact with Pol III but is instead attributable to another reason. Moreover, we found that the mutant β^{E202K} clamp binds more strongly to Pol III than the wild-type clamp (Table 1 and 2). We attribute its inability to impede growth when expressed at an elevated cellular level to a different mechanism than the "failure-to-sequester" mechanism of the other clamp mutants described in this report. Further analysis of the *dnaN*^{E202K} strain determined that it expresses an elevated cellular level of the *nrdAB*-encoded class 1a ribonucleotide reductase, which also suppresses the growth defect (58). Thus, inhibition of growth caused by an elevated level of the wild-type clamp can be alleviated through dissimilar mechanisms.

We demonstrated previously that in the absence of DNA, Pol IIIα retains the ability to bind to a β clamp lacking both hydrophobic clefts, albeit binding affinity is ~10-fold weaker (44), which is consistent with the idea that Pol IIIα makes additional contacts with the clamp that were not captured in the cryo-EM structure. Additional structural and functional studies are required to determine whether the substitutions examined in this work target clamp residues involved in the direct interaction with Pol III or whether they affect the structure of the clamp to indirectly affect its interaction with Pol III. However, our finding that β^{E202K} and the wild-type clamp bound Pol II and Pol IV with similar binding kinetics (Table 3) and that the β^{E202K} and its wild-type counterpart supported comparable levels of Pol II and Pol IV replication (Fig. 3B and C) argues that the E202K mutation likely fails to significantly change the clamp structure. Regardless of the mechanistic basis of the effect of the E202K mutation on β clamp structure/function, this work suggests strongly that interactions of the β clamp with Pol III are more extensive than those appreciated currently based on results of X-ray crystallography and cryo-EM experiments (34, 36).

As mentioned above, β^{E202K} retained its ability to stimulate replication by Pol II and Pol IV (Fig. 3), which suggests strongly that the mutant protein is loaded onto DNA *in*

vitro by the DnaX clamp loader complex but is defective in stimulating DNA replication by Pol III. How is the mutant clamp able to sustain *E. coli* viability? As an explanation, the β^{E202K} mutant supported Pol III replication at a range of concentrations from 20 to 60 nM (Fig. 3A and 4 inset), which is ≥4-fold below the measured intracellular β clamp concentration of ~250 to 550 nM (59, 60). Apparently, the chromosomally expressed level of β^{E202K} can compensate for its biochemical defect. A similar situation appears to explain the modest phenotypes of a *dnaN159* mutant (40), which shows near-normal growth of *E. coli* at 30°C despite the severe defect of the mutant clamp in supporting Pol III replication *in vitro* (42). Furthermore, we determined recently that a *dnaN*^{E202K} strain expresses elevated levels of the *nrdAB*-encoded class 1A ribonucleotide reductase (RNR) (58). Because overexpression of RNR increases cellular deoxynucleoside triphosphate (dNTP) levels (61, 62), which increases the rate of Pol III replication (63), the elevated RNR levels in the *dnaN*^{E202K} strain may help to alleviate its replication defect by increasing the rate of Pol III replication. We suggest that this condition helps with viability and explains why the SOS response is induced only modestly.

Both the Pol IIIα catalytic (K_D, ~100 nM) and Pol IIIε proofreading subunits (K_D, ~200 μM) bind the clamp cleft using independent CBMs (36). SPR experiments of the current work indicate that β^{E202K} is altered in its interaction with the Pol III$\alpha\varepsilon\theta$ complex (Table 1). Specifically, β^{E202K} displays an ~7-fold lower K_{D1} (2.20 ± 0.56 nM versus 15.3 ± 7.67 nM) and an ~4-fold higher K_{D2} (204.8 ± 3.70 nM versus 56.7 ± 22.2 nM) than the wild-type clamp. Hence, the E202K mutation increases the affinity of the clamp for Pol IIIα while reducing its affinity for Pol IIIε. Consistent with this conclusion, BLI experiments confirmed that β^{E202K} has an ~3-fold higher affinity for Pol IIIα than the wild-type clamp (Table 2). These small differences in binding affinities between the mutant and wild-type clamp are in contrast with the more pronounced defect of β^{E202K} in supporting Pol III-dependent DNA replication (Fig. 3A and 4). We interpret these results to suggest that interactions of the β clamp with Pol III are more dynamic than appreciated currently; the E202K mutation may interfere with these dynamics to explain the impaired ability of the mutant clamp protein to stimulate Pol III replication *in vitro* (Fig. 3A and 4). Consistent with this model, we determined recently that the *dnaN*^{E202K} strain failed to exhibit an elevated spontaneous frequency of Rif^r, despite the fact that this strain expresses an elevated cellular abundance of RNR (58).

Figure 10 provides an updated view of the clamp surfaces identified in this work that contribute to its function with various *E. coli* Pols, as well as the locations of clamp surfaces involved in these interactions identified in previous work (12, 26, 34, 36, 64). Importantly, while some surfaces, such as the clamp's hydrophobic cleft, are used by all known clamp partners, others are suggested to be specific for discrete Pols. For example, based on cryo-EM, loop residues, ^{24}RPTLP^{28} and ^{275}NEKF^{278} are suggested to interact with Pol IIIα when it is assembled on primed DNA (36). Likewise, replacement of residues ^{148}HGDVR^{152} with five consecutive alanine residues impedes the action of Pol II and Pol IV, as well as the ability of the clamp to be loaded onto DNA, without affecting its ability to stimulate Pol III replication (12). Finally, residues E93 and L98, which are located on the clamp rim, are dispensable for Pol IV replication but play a vital role in helping to recruit Pol IV to the replication fork (64, 65). Despite all five *E. coli* Pols contacting the clamp cleft, results with P363S (Fig. 3A) suggest there are differences in how Pol II interacts with the clamp cleft compared with Pols III and IV (Fig. 10). Furthermore, our finding that D150N and G157S are impaired for stimulating Pol III replication *in vitro* (Fig. 3A) indicates that residues ^{148}HGDVR^{152}, as well as an adjacent surface, also contribute to Pol III function. Interestingly, the G157S substitution affects these three Pols differently; while this mutant is impaired for stimulating Pol III, it fails to interfere with Pol II replication and it actually stimulates Pol IV replication compared with the wild-type clamp (Fig. 10). Likewise, the D150N substitution fails to interfere with Pol II replication *in vitro*, suggesting that this Pol interacts with residues ^{148}HGDVR^{152} differently compared with Pol III and Pol IV. Finally, it is interesting that Q61K and S107L are impaired for stimulating Pol IV replication *in vitro* since they are

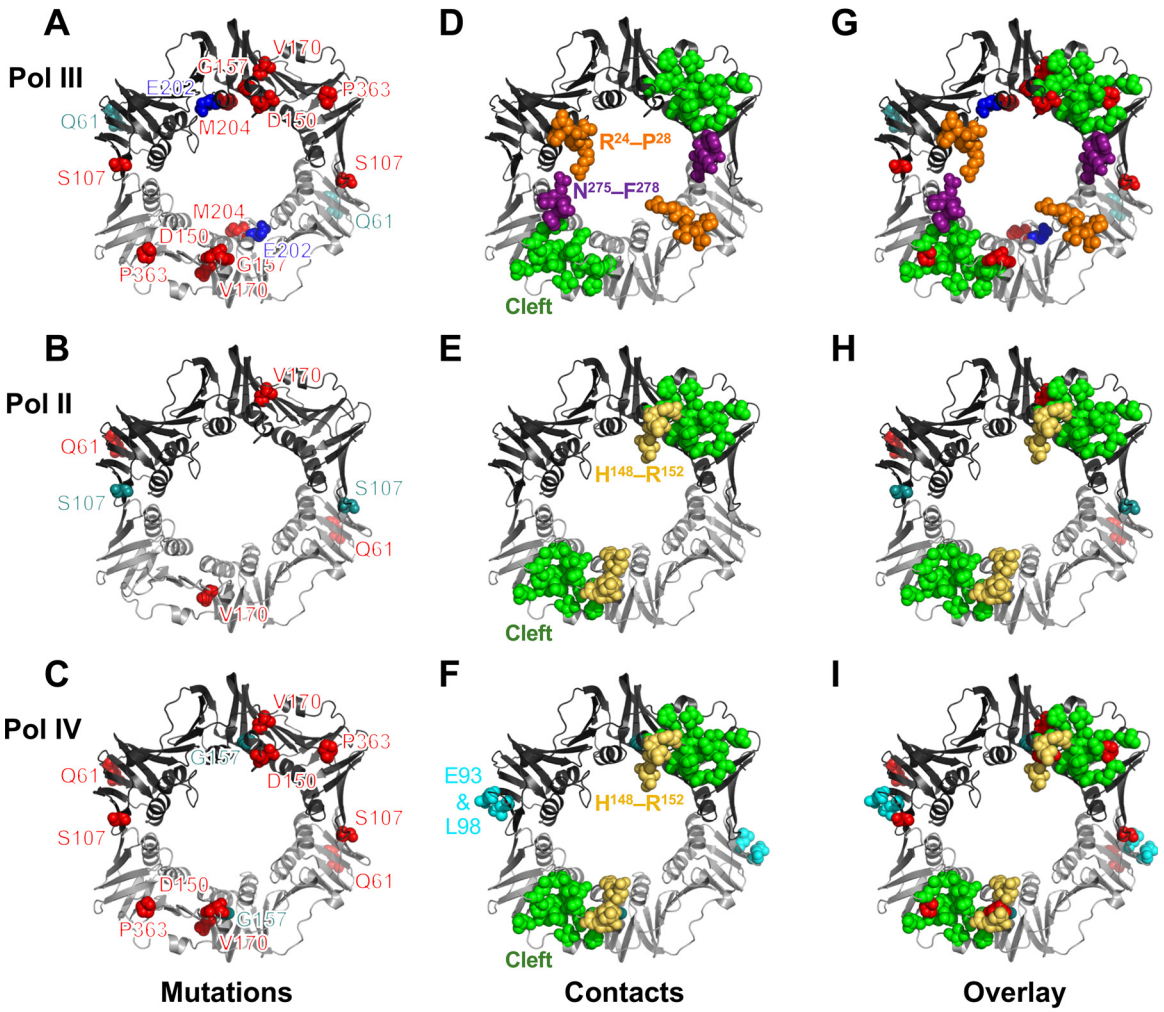

FIG 10 β Clamp residues important for supporting the replication activity of Pol III, Pol II, and Pol IV. The positions of amino acid substitutions determined in this work to be impaired in stimulating the replication activity *in vitro* of Pol III (A), Pol II (B), or Pol IV (C) are shown relative to the X-ray crystal structure of the β clamp (PDB: 1MMI). Residue E202 (dark blue) when substituted with Lys leads to an increased affinity of the β clamp for Pol III compared with the wild-type clamp. Residues Q61, S107, and G157 (teal) when substituted stimulate replication by Pol III, Pol II, and Pol IV, respectively, compared with the wild-type clamp. The positions of the other mutations that were impaired for supporting Pol III, Pol II, and/or Pol IV replication are shown in red. The positions of clamp surfaces known to contact Pol III (D), Pol II (E), or Pol IV (F) are indicated, including the clamp's hydrophobic cleft (green). Residues ^{24}RPTLP^{28} (orange) and ^{275}NEKF^{278} (purple), which are based on the cryo-EM structure, are suggested to interact with Pol IIIα when bound to primed DNA (36); residues ^{148}HGDVR^{152} (yellow) are dispensable for Pol III replication but interact with and are required for Pol II and Pol IV replication *in vitro* (12); and residues E93 and L98K (light blue), which are located on the clamp rim, help to recruit Pol IV to the replication fork. Positions of amino acid substitutions altered for interaction with Pol III (G), Pol II (H), or Pol IV (I) are superimposed on clamp surfaces known to interact with these respective Pols. These images were generated using PyMOL v2.4.0.

near residues E93 and L98 that are thought to help recruit Pol IV to the replication fork rather than stimulate Pol IV replication. Thus, the clamp surface defined by these residues may also play a role in supporting Pol IV replication. In summary, the genetic assay that was used to identify the mutants discussed in this work could prove to be a powerful tool for mapping functional surfaces of the clamp required for managing its different partner proteins. Further analyses of these and other mutant clamp proteins are likely to broaden our understanding of β clamp function.

MATERIALS AND METHODS

Pol III$\alpha\varepsilon\theta$-β-DNA and δ-β-DNA structural models. Structural models were built using PyMOL (Schrödinger). The Pol III$\alpha\varepsilon\theta$-β-DNA model is based on the cryo-EM structure of the *E. coli* Pol IIIα-Pol IIIε-DnaXτ_C complex bound to DNA (PDB: 5FKW) (36). Using a previously published model of Pol III$\alpha\varepsilon\theta$-β-DNA derived from X-ray scattering, cross-linking, and nuclear magnetic resonance (NMR) (57), Pol III$\varepsilon\theta$ was

extracted and aligned with the cryo-EM structure (PDB: 5FKW) using ε as the subject. This alignment permitted a prediction of how the θ subunit may be positioned within this complex. Pol IIIα residues Ala^{928}-Asp^{1160} are not shown in the cryo-EM structure of the Pol IIIα-Pol IIIε-DnaXτ_C-DNA complex (PDB: 5FKW). To model the full-length Pol IIIα protein, the full-length structure of Pol IIIα described by Ozawa et al. (57) was extracted and superimposed onto the portion of Pol IIIα present in the cryo-EM complex (PDB: 5FKW).

The δ-β-DNA model is based on the model of the $\delta^{1\text{-}140}$-$\beta^{I272A,\ L273A}$ (β monomer) complex (34). The β protomer present in this structure (PDB: 1JQL) was aligned to β clamp in the cryo-EM structure of the Pol IIIα-Pol IIIε-DnaXτ_C-DNA complex (PDB: 5FKW), and Pol III$\alpha\varepsilon\theta$ and DnaXτ_C were hidden. The crystal structure of $\delta^{1\text{-}140}$-β contains only the N-terminal 140 residues of δ; residues Thr^{141}-Gly^{343} are absent. We therefore aligned the larger fragment of δ lacking only its C-terminal 5 residues (^{339}VFIDG^{343}) from the crystal structure of the processivity clamp loader γ complex (PBD: 1JR3) onto the $\delta^{1\text{-}140}$-β complex.

DNAs and proteins. The supercoiled *oriC*-containing plasmid M13*oriC*2LB5 was a laboratory stock (66). Plasmid pRM115 was built by sequentially inserting BglII-BamHI fragments containing the T7 promoter and the coding sequence for Pol IIIα (pRM108) (42) and Pol IIIε (pRM109) (42), respectively, into the pET16b derivative containing the coding sequence for N-terminally His$_{10}$-tagged Pol IIIθ. All three genes are transcribed in the same direction, and each gene is expressed from its own T7 promoter. Plasmid pPolIIIα^{HMK} was constructed by replacing the NdeI-BamHI *dnaN* fragment in pβ^{HMK} (67) with the NdeI-BamHI fragment from pRM108 (42) encoding the Pol IIIα subunit.

The $\tau_2\gamma\delta\delta'\psi\chi$ form of the DnaX clamp loader complex (5); the γ form of the DnaX clamp loader complex ($\gamma_3\delta\delta'$) (21); untagged and N-terminally His$_6$-tagged forms of the wild-type β, β^{E202K}, and β^C clamps (29); the untagged δ subunit of the DnaX complex (42); and untagged Pol III core (Pol III$\alpha\varepsilon\theta$), Pol II (42), and Pol IV (65); as well as other replication proteins were each purified as described (12, 42, 43, 65). Pol IIIα^{HMK} was purified using HisTrap high performance (HP) chromatography (GE Healthcare) followed by chromatography on MonoQ and HiTrap Heparin HP columns (GE Healthcare). The Pol III core in which the θ subunit bore an N-terminal His$_{10}$-tag (Pol III$\alpha\varepsilon\theta^{His}$) was purified using the same procedure as the untagged Pol III core with the addition of a final HisTrap HP step (42). The concentration of each purified protein was determined by the dye binding method (68) and also by densitometric analysis of SDS-PAGE analysis after staining with Coomassie blue using bovine serum albumin (BSA) to prepare a standard curve.

Primer extension assays. Reactions (20 μl) contained replication assay buffer (20 mM Tris-HCl [pH 7.5], 8.0 mM $MgCl_2$, 0.1 mM EDTA, 5 mM dithiothreitol [DTT], 1 mM ATP, 5% glycerol, and 0.8 mg/ml BSA), 0.133 mM dNTPs containing [methyl-^{3}H]dTTP (49 cpm/pmol of total nucleotide), 2 mM single-stranded DNA binding protein (SSB), and 5 nM M13 ssDNA annealed to an oligonucleotide primer (SP20, 5′-ACG CCT GTA GCA TTC CAC AG-3′; Sigma Genosys). Reactions were initiated by the addition of 20 nM wild-type or β^{E202K} clamp protein, 10 nM of either the τ ($\tau_2\gamma\delta\delta'\psi\chi$; used with Pol III) or γ ($\gamma_3\delta\delta'$; used with Pol II and Pol IV) form of the DnaX clamp loader complex, and the indicated Pol (1 nM Pol III, 1 nM Pol II, or 10 nM Pol IV). Reactions were quenched by the addition of 1 ml of 15% trichloroacetic acid and 0.1 M sodium pyrophosphate, followed by incubation on ice for 15 min. The acid-insoluble DNA was collected onto 2.4-cm glass microfiber filters (VWR) by vacuum filtration, and nucleotide incorporation was quantified by liquid scintillation spectroscopy as described (42).

***oriC*-dependent DNA replication assays.** DNA replication assays contained 40 mM HEPES-KOH (pH 7.6); 20 mM Tris-HCl (pH 7.5); 10 mM magnesium acetate; 4 mM DTT; 0.08 mg/ml BSA; 4% (wt/vol) sucrose; 2 mM ATP; 0.5 mM (each) CTP, GTP, and UTP; 0.1 mM (each) dATP, dCTP, dGTP, and [methyl-^{3}H] dTTP (25 to 30 cpm/pmol); 40 mM phosphocreatine; creatine kinase (200 μg/ml); M13*oriC*2LB5 (200 ng; 46 fmol); SSB (4 pmol); HU (0.3 pmol); DNA gyrase A subunit (3.8 pmol); DNA gyrase B subunit (5.8 pmol); DnaB (0.3 pmol as hexamer); DnaC (2 pmol) and primase (0.2 pmol); DnaA (110 ng; 2 pmol); Pol III* (i.e., Pol III HE lacking β clamp; 90 ng; 0.18 pmol); and the indicated amount of the β or β^{E202K} clamp in a volume of 25 μl. After the mixtures were incubated for 20 min at 30°C, DNA replication was measured as described above.

Surface plasmon resonance (SPR) experiments. SPR experiments were conducted at 25°C using a dual-channel Reichert SR7500DC instrument. All experiments were carried out in HEPES-buffered saline supplemented with EDTA and polysorbate 20 (HBS-EP) buffer (10 mM HEPES [pH 7.4], 150 mM NaCl, 3 mM EDTA, and 0.005% Tween 20). Approximately 4,000 response units (RU) of the penta-His antibody (Qiagen) were covalently captured on a 500-kDa carboxymethyl dextran chip (Reichert, Inc.) by amine coupling to both channels as per the manufacturer's recommendation. Approximately 1,000 RU of each N-terminally His$_6$-tagged ligand (β-His$_6$, β^{E202K}-His$_6$, or Pol III$\alpha\varepsilon\theta$-His$_6$) was captured in the left channel for 3 min at a flow rate of 25 μl/min, and 250 to 4,000 nM δ or 62.5 to 1,000 nM β or β^{E202K} (analyte) was flowed over both the left and the right channels for 1.5 min at a flow rate of 25 μl/min. Interactions were measured using a kinetic titration approach in which increasing concentrations of the analyte were injected sequentially over both channels (69). The chip surface was regenerated between each kinetic titration using a regeneration cocktail flowed over both channels for 45 sec at 25 μl/min as described (70). Kinetic constants were determined using Scrubber 2.0c (Biologic Software Pty, Australia) and ClampXP 3.50 software provided by Reichert (71).

Biolayer interferometry (BLI) experiments. BLI experiments were conducted at 25°C using a FortéBio Octet RED 96e instrument (Sartorius). All experiments were carried out in HBS-EP buffer using FortéBio Penta-His (HIS1K) Dip and Read biosensors. Biosensor tips were hydrated for 10 min in HBS-EP buffer and allowed to equilibrate to obtain a stable baseline in HBS-EP buffer for 1 min prior to loading N-terminally His$_6$- and heart muscle kinase-tagged ligands (300 nM [for β or β^{E202K}] or 1,000 nM [for β^C] Pol IIIα, or 1,000 nM Pol II or Pol IV). Following ligand capture, biosensors were quenched in SuperBlock (Thermo Scientific) and EZ-Link biocytin (50 μM; Thermo Fisher Scientific) for 5 min and allowed to reach a stable baseline again for 3 min. The untagged analyte (β^C, β^+, or β^{E202K}) was then allowed to associate

TABLE 6 *E. coli* strains and plasmids

Strain or plasmid	Relevant genotype or characteristic	Source
Strains		
MC4100	[*araD139*]$_{B/r}$ Δ(*argF-lac*)*169 flhD5301* Δ(*fruK-yeiR*)*725* (*fruA25*) *relA1 rpsL150* (Str^R) *rbsR22* Δ(*fimB-fimE*)*632*(::IS*1*) *deoC1*	M. O'Brian
MG1655	*ilvG* mutant *rfb-50 rph-1*	*E. coli* Genetic Stock Center
VB001	MG1655 *dnaN*$^+$-*tet*$^+$-*recF*$^+$	61
VB019	MG1655 *dnaN*^{E202K}-*tet*$^+$-*recF*$^+$	This work
VB023	MG1655 *dnaN*$^+$-*tet*$^+$-*recF*$^+$ Δ*dinB749*::*kan*	This work
VB024	MG1655 *dnaN*^{E202K}-*tet*$^+$-*recF*$^+$ Δ*dinB749*::*kan*	This work
MS105	*rpsL31 xyl-5 mtl-1 galK2 lacY1 tsx-33 supE44 thi-1 hisG4*(Oc) *argE3*(Oc) *araD139 thr-1* Δ(*gpt-proA*)*62 sulA211 lexA51*(Def) *dnaN159 tnaA300*::Tn*10*	40
CH100	MS105 *dnaN*$^+$-*tet*$^+$-*recF*$^+$	This work
CH101	MS105 *dnaN*^{E202K}-*tet*$^+$-*recF*$^+$	This work
Plasmids		
pβ^{HMK}	Amp^r; pET16b derivative that expresses the β clamp bearing N-terminal His$_6$ and heart muscle kinase (HMK) tags	67
pβE202K^{HMK}	Amp^r; pET16b derivative that expresses the β^{E202K} clamp bearing N-terminal His$_6$ and heart muscle kinase (HMK) tags	This work
pJRC210	Amp^r; pBR322 derivative that overexpresses the β clamp from the *tac* promoter	C. McHenry (33)
pJRCβΔ362-6	Amp^r; pBR322 derivative that expresses β^C (lacking its C-terminal five residues) from the *tac* promoter	44
pJRCHA4.1	Amp^r; pBR322 derivative that expresses β^{Q61K} from the *tac* promoter	33
pJRCHA5.1	Amp^r; pBR322 derivative that expresses β^{S107L} from the *tac* promoter	33
pJRCHA8.1	Amp^r; pBR322 derivative that expresses β^{D150N} from the *tac* promoter	33
pJRCHA5G11	Amp^r; pBR322 derivative that expresses β^{G157S} from the *tac* promoter	33
pJRCHA8I11	Amp^r; pBR322 derivative that expresses β^{V170M} from the *tac* promoter	33
pJRCHA7.1	Amp^r; pBR322 derivative that expresses β^{E202K} from the *tac* promoter	33
pJRCHA6F11	Amp^r; pBR322 derivative that expresses β^{M204K} from the *tac* promoter	33
pJRCHA6.2	Amp^r; pBR322 derivative that expresses β^{P363S} from the *tac* promoter	33
pRM115	Amp^r; pET16b derivative that overexpresses Pol III core bearing a His-tagged Pol IIIθ subunit (Pol III$\alpha\varepsilon\theta$-His$_{10}$) from the T7 promoter	This work
pPolIIIα^{HMK}	Amp^r; pET16b derivative that overexpresses Pol IIIα bearing a His$_6$ and heart muscle kinase tag at its N terminus from the T7 promoter	This work
pET15b-*dnaX*	Amp^r; pET15b derivative lacking the His$_6$ tag that overexpresses the τ and γsubunits of the DnaX clamp loader complex from the T7 promoter	L. Bloom
pET15b-*holA*	Amp^r; pET15b derivative lacking the His$_6$ tag that overexpresses the δ subunit of the DnaX clamp loader complex from the T7 promoter	L. Bloom
pET15b-*holB*	Amp^r; pET15b derivative lacking the His$_6$ that overexpresses the (δ' subunit of the DnaX clamp loader complex) from the T7 promoter	L. Bloom
pET15b-*holCD*	Amp^r; pET15b derivative lacking the His$_6$ tag that overexpresses the ψ and χ subunits of the DnaX clamp loader complex from the T7 promoter	L. Bloom
pRM107	Amp^r; pET11a derivative that overexpresses Pol II from the T7 promoter	42
pRM112	Amp^r; pET11a derivative that overexpresses Pol IV from the T7 promoter	42
pKD46	Amp^r; pSC101 *oriV* with *repA101*(Ts) mutation; expresses λRed recombinase from the *araBAD* promoter	72
pANTF	Kan^r, Tet^r; p15A *oriV*; encodes "*dnaA-dnaN*$^+$-*tet-recF*" cassette	12
pAN(E202K)TF	Kan^r, Tet^r; pANTF derivative that encodes "*dnaA-dnaN*^{E202K}-*tet-recF*" cassette; for diagnostic purposes, the *dnaN*^{E202K} allele additionally contains a disrupted PvuII restriction site	This work
pWSK29	Amp^r; pSC101-derived plasmid	78
pRM100	Amp^r; pWSK29 derivative that bears *polA*$^+$ (Pol I) expressed from its native promoter	54
pRM101	Amp^r; pWSK29 derivative that bears *polB*$^+$ (Pol II) expressed from its native promoter	54
pRM102	Amp^r; pWSK29 derivative that bears *dinB*$^+$ (Pol IV) expressed from its native promoter	54
pRM103	Amp^r; pWSK29 derivative that bears *umuD'-umuC*$^+$ (Pol V) expressed from their native promoter	54

for 3 min at increasing concentrations (100, 200, 400, 600, 800, and 1,000 nM wild-type β or β^{E202K} or 400, 600, 800, 1,000, 5,000, 5,500, 6,000, and 6,500 nM β^C for Pol IIIα; 93.5, 157.5, 375, 750, 1,500, and 3,000 nM wild-type β or β^{E202K} for Pol II; 31.25, 62.5, 125, 250, and 500 nM wild-type β for Pol IV or 250, 500, and 1,000 nM β^{E202K} for Pol IV) to individual biosensors before dissociation was monitored for 3 min. Binding kinetics were then analyzed using FortéBio data analysis HT software (v12.0.2.59; Molecular Devices LLC). Reference biosensors were also utilized to measure background and nonspecific binding.

Bacteriological techniques. *E. coli* strains and plasmid DNAs are described in Table 6. Site-directed mutagenesis was performed using the QuikChange mutagenesis kit (Agilent Technologies). Plasmids

were transformed into the indicated strains using $CaCl_2$ treatment as described previously (40). Unless otherwise noted, strains were cultured in Luria-Bertani medium (LB; 10 g/liter tryptone, 5 g/liter yeast extract, and 10 g/liter NaCl). When appropriate, the following antibiotics were used at the indicated concentrations: ampicillin (Amp), 150 μg/ml; kanamycin (Kan), 40 μg/ml; tetracycline (Tet), 10 μg/ml for strains bearing plasmids or 2.5 μg/ml for strains bearing the chromosomal *tet* allele between *dnaN* and *recF*; and rifampicin (Rif), 50 μg/ml.

Construction of the *dnaN*^{E202K} *E. coli* strain. The chromosomal *dnaN*$^{+}$ gene was replaced with the *dnaN*^{E202K} allele by phage λ-Red recombineering (72). Briefly, the E202K mutation was introduced into plasmid pANTF (12, 32) using the QuikChange method (Agilent Genomics) per the manufacturer's recommendations with primers BetaE202K top (CGTAAAGGCGTGATTAAACTGATGCG) and BetaE202K bottom (GCATACGCATCAGTTTAATCACGCCT). In a second QuikChange reaction, we introduced a silent mutation that disrupts a PvuII site in *dnaN* for use as a diagnostic tool to screen for the presence of the E202K mutation as described (12). The resulting plasmid was named pAN(E202K)TF. Phage λ-mediated recombination was used to replace the wild-type *dnaN*$^{+}$ locus with the 3,941-bp "*dnaA-dnaN*^{E202K}*-tet*$^{+}$*-recF*" cassette that was PCR amplified from pAN(E202K)TF using primers JK28 + 2 and RecF back (12, 32). Importantly, the *tet* insertion between *dnaN* and *recF* fails to exert a polar effect on *recF* (12, 32). The gel-purified DNA fragment was electroporated into strain MC4100 bearing plasmid pKD46, which expresses a λ recombinase function under the control of the *araBAD* promoter (72), using a Bio-Rad gene pulser (2.5 kV, 25 μF, and 200 Ω) equipped with 0.2-cm cuvettes (Bio-Rad). Recombinants resulting from double crossover were selected at 30°C on LB plates containing 2.5 μg/ml tetracycline. The genotype of the recombinant strain was confirmed by diagnostic PCR using primers DnaAP and RecF bottom (12, 32) and by DNA sequence analysis of the entire "*dnaA-dnaN*^{E202K}*-tet*$^{+}$*-recF*" cassette (Biopolymer Facility, Roswell Park Cancer Institute). An Amp^{s} isolate lacking plasmid pKD46 was obtained by plating at 42°C. The *dnaN*^{E202K} allele was introduced into MG1655 using P1*vir* transduction, resulting in strain VB019. Likewise, the isogenic wild-type *dnaN* allele linked to *tet* (*dnaA-dnaN*$^{+}$*-tet-recF*) was transduced into MG1655, resulting in strain VB001 (61).

Quantitative Western blot analysis. Saturated overnight cultures were grown at 37°C and subcultured 1:100 in LB medium to an OD_{600} of ~0.5. For each strain, the volume equivalent of 2 ml of an OD_{600} of 0.5 culture was centrifuged, and the cell pellet was resuspended in 15 μl bacterial protein extraction reagent (B-PER) (Pierce) plus 35 μl SDS loading dye (63 mM Tris-HCl [pH 6.8], 10% glycerol, 2% SDS, 0.005% bromophenol blue, and 10% 2-mercaptoethanol). Samples (30 μl) were heated to 95°C for 10 minutes and separated using 10-well 4% to 20% Mini-Protean TGX precast protein gels (Bio-Rad). Proteins were transferred to polyvinylidene difluoride (PVDF) membranes using a Trans-Blot Turbo semi-dry transfer system (Bio-Rad). Protein transfer was verified by staining each membrane with Ponceau S stain (Sigma) for 5 minutes followed by washing with water prior to imaging. The Ponceau S stain was removed from the membrane by washing with 0.1 M NaOH. The membranes were washed first with 1× Tris-saline (TS; 150 mM NaCl and 50 mM Tris-HCl [pH 7.6]) and then with 1× TS plus Tween (0.05%). Membranes were blocked with 1× TS plus Tween (0.05%) plus 2% nonfat dry milk for 1 h prior to incubation with the primary anti-β clamp polyclonal antibody overnight at 4°C (1:50,000). The anti-β clamp polyclonal antibody, which was generated using a University at Buffalo IACUC-approved protocol, was described previously (58). Membranes were washed with 1× TS plus Tween (0.05%) and probed with secondary goat anti-rabbit antibody (Bio-Rad) at 1:25,000 for 1.5 h at room temperature. Membranes were washed and then treated with Clarity Western enhanced chemiluminescence (ECL) substrate for 2 minutes prior to imaging on a ChemiDoc Imager (Bio-Rad). Quantitation of each protein was determined using the Quantity Tools feature on Bio-Rad ImageLab software. The average protein levels reported were determined from at least 2 independent experiments.

Quantitative PCR (qPCR). For quantitative analysis of mRNA levels, cells were grown in LB media seeded with 1:1,000 dilutions of overnight cultures to mid-exponential phase at 37°C. After mRNA purification by phenol-chloroform extraction (73), cDNA was prepared using a Bio-Rad Iscript cDNA synthesis kit as per the manufacturer's recommendation. Genomic DNA was extracted from the parent MG1655 strain for use as a primer control. qPCR was performed in the Bio-Rad iCycler, and starting quantity (SQ) values were calculated from the threshold cycle (C_T) values after fitting to the standard curve obtained using genomic DNA standards. To control for loading variations among samples, the SQ values were normalized to *hcaT* levels similarly determined by qPCR. qPCR primer pairs and their sequences were as follows: qSulAFor (forward primer for *sulA* transcript), 5′-GGTTGGTTGGCAGATGAT-3′; qSulARev (reverse primer for *sulA* transcript), 5′-GCTTACCGGACGCATAATAA-3′; qLexAFor (forward primer for *lexA* transcript), 5′-CAGGTCGATCCTTCCTTATTC-3′; and qLexARev (reverse primer for *lexA* transcript), 5′-CAGCAA GTCACCATCCATAA-3′.

Ratios of *oriC* to *TerC* (*oriC*/*TerC*) were measured as described previously (61, 73) using the following primers: oriC_1 (forward primer for *oriC*), 5′-CTGTGAATGATCGGTGATCC-3′; oriC_2 (reverse primer for *oriC*), 5′-AGCTCAAACGCATCTTCCAG-3′; terC_1 (forward primer for *TerC*), 5′-CAGAGCGATATATCACAGCG-3′; and terC_2 (reverse primer for *TerC*), 5′-TATCTTCCTGCTCAACGGTC-3′.

Whole-transcriptome analysis. A whole-transcriptome analysis was performed on three biological replicates of each strain by the UB Genomics and Bioinformatics Core as described previously (61). Briefly, RNA was isolated from exponential-phase cultures grown at 37°C using phenol-chloroform (73). Purified RNA was depleted of the rRNA using the bacterial Ribo-Zero rRNA removal kit (Illumina) as per the manufacturer's recommendations. The quality of each rRNA-depleted RNA sample was examined using a bioanalyzer prior to its use in RNA-seq as rapid 100-cycle single-read sequencing using the Illumina next-generation sequencer. Generation of fragments per kilobase per million (FPKM) was

performed using Cufflinks 2.1.1. Results for the wild-type control were published previously (58) but are part of the same data set as the *dnaN*^{E202K} strain included here.

Flow cytometry. Genome content after replication run-out was measured by flow cytometry as described previously with some modifications (74). Briefly, cells were grown at 37°C with aeration in M9 minimal media supplemented with glucose and Casamino Acids to an OD_{600} of 0.1 to 0.2, at which point rifampicin and cephalexin were added to a final concentration of 300 μg/ml and 15 μg/ml, respectively. Cultures were incubated at 37°C with aeration for 4 h. Each culture (1 ml) was then mixed with 9 ml of 70% ethanol. Fixed cells were pelleted and resuspended in 1 ml of PBS containing 0.5 μl SYTOX green (Life Technologies) and analyzed using a BD fluorescence-activated cell sorter (FACS) Canto instrument and FlowJo 10.2 software.

Measurements of sensitivity to DNA damaging agents and DNA damage-induced mutagenesis. To measure sensitivity to DNA damaging agents, overnight cultures were subcultured 1:1,000 and grown at 37°C until at an OD_{600} of ~0.5 for analysis of MMS and UV sensitivity. Cultures were normalized to a volume of 1 ml of an OD_{600} of 0.5 in 0.8% saline. To measure MMS sensitivity, samples were serially diluted in 0.8% saline and spotted onto LB agar plates containing the indicated concentrations of MMS. Plates were then incubated overnight at 37°C and subsequently imaged. To measure UV sensitivity, samples were serially diluted in 0.8% saline, spotted onto LB agar plates, and allowed to dry. Experimental plates were exposed to UV light for various lengths of time. Plates were then incubated overnight at 37°C and subsequently imaged. The frequency of rifampicin-resistant mutations induced by MMS or UV was measured as described previously (40, 75, 76).

Data availability. The RNA-seq data discussed in this report have been deposited in NCBI Gene Expression Omnibus (77) and are accessible through GEO Series accession number GSE175936.

ACKNOWLEDGMENTS

We thank Phillip Page (Reichert Technologies, Life Sciences) for advice with kinetic analysis of SPR sensorgrams, Julia Grimwade (Florida Institute of Technology) for advice with flow cytometry, Mark O'Brian (University at Buffalo, SUNY) for *E. coli* strain MC4100, Linda Bloom (University of Florida) for *E. coli* DnaX clamp loader subunit overproducers, Charles McHenry (University of Colorado, Boulder) for plasmid pJRC210, Jessica Sutton for help with formatting the figures, and the members of our labs for helpful discussions.

Public Health Service Awards R01 GM066094 (M.D.S.), R01 GM130761 (M.D.S.), R01 GM130761-02S1 (M.D.S.), and R01 GM090063 (J.M.K.) from the National Institutes of Health, NIGMS supported this work. The funders had no role in study design, data collection or analysis, decision to publish, or the preparation of the manuscript.

We have no conflicts of interest to declare.

REFERENCES

1. Georgescu RE, Kim SS, Yurieva O, Kuriyan J, Kong XP, O'Donnell M. 2008. Structure of a sliding clamp on DNA. Cell 132:43–54. https://doi.org/10.1016/j.cell.2007.11.045.
2. Kong XP, Onrust R, O'Donnell M, Kuriyan J. 1992. Three-dimensional structure of the beta subunit of *E. coli* DNA polymerase III holoenzyme: a sliding DNA clamp. Cell 69:425–437. https://doi.org/10.1016/0092-8674(92)90445-l.
3. Stukenberg PT, Studwell-Vaughan PS, O'Donnell M. 1991. Mechanism of the sliding beta-clamp of DNA polymerase III holoenzyme. J Biol Chem 266:11328–11334. https://doi.org/10.1016/S0021-9258(18)99166-0.
4. Friedberg EC, Walker GC, Siede W, Wood RD, Schultz RA, Ellenberger T. 2006. DNA repair and mutagenesis, 2nd ed. American Society of Microbiology, Washington DC.
5. Pritchard AE, Dallmann HG, Glover BP, McHenry CS. 2000. A novel assembly mechanism for the DNA polymerase III holoenzyme DnaX complex: association of deltadelta' with DnaX(4) forms DnaX(3)deltadelta'. EMBO J 19:6536–6545. https://doi.org/10.1093/emboj/19.23.6536.
6. Xiao H, Naktinis V, O'Donnell M. 1995. Assembly of a chromosomal replication machine: two DNA polymerases, a clamp loader, and sliding clamps in one holoenzyme particle. IV. ATP-binding site mutants identify the clamp loader. J Biol Chem 270:13378–13383. https://doi.org/10.1074/jbc.270.22.13378.
7. Blinkowa AL, Walker JR. 1990. Programmed ribosomal frameshifting generates the *Escherichia coli* DNA polymerase III gamma subunit from within the tau subunit reading frame. Nucleic Acids Res 18:1725–1729. https://doi.org/10.1093/nar/18.7.1725.
8. Dohrmann PR, Correa R, Frisch RL, Rosenberg SM, McHenry CS. 2016. The DNA polymerase III holoenzyme contains gamma and is not a trimeric polymerase. Nucleic Acids Res 44:1285–1297. https://doi.org/10.1093/nar/gkv1510.
9. McInerney P, Johnson A, Katz F, O'Donnell M. 2007. Characterization of a triple DNA polymerase replisome. Mol Cell 27:527–538. https://doi.org/10.1016/j.molcel.2007.06.019.
10. Davey MJ, Jeruzalmi D, Kuriyan J, O'Donnell M. 2002. Motors and switches: AAA+ machines within the replisome. Nat Rev Mol Cell Biol 3:826–835. https://doi.org/10.1038/nrm949.
11. Park MS, O'Donnell M. 2009. The clamp loader assembles the beta clamp onto either a 3' or 5' primer terminus: the underlying basis favoring 3' loading. J Biol Chem 284:31473–31483. https://doi.org/10.1074/jbc.M109.050310.
12. Heltzel JM, Scouten Ponticelli SK, Sanders LH, Duzen JM, Cody V, Pace J, Snell EH, Sutton MD. 2009. Sliding clamp-DNA interactions are required for viability and contribute to DNA polymerase management in *Escherichia coli*. J Mol Biol 387:74–91. https://doi.org/10.1016/j.jmb.2009.01.050.
13. Nanfara MT, Babu VM, Ghazy MA, Sutton MD. 2016. Identification of beta clamp-DNA interaction regions that impair the ability of *E. coli* to tolerate specific classes of DNA damage. PLoS One 11:e0163643. https://doi.org/10.1371/journal.pone.0163643.
14. Burgers PM, Kornberg A, Sakakibara Y. 1981. The *dnaN* gene codes for the beta subunit of DNA polymerase III holoenzyme of *Escherichia coli*. Proc Natl Acad Sci U S A 78:5391–5395. https://doi.org/10.1073/pnas.78.9.5391.
15. Kurth I, O'Donnell M. 2009. Replisome dynamics during chromosome duplication. EcoSal Plus 3:10.1128/ecosalplus.4.4.2. https://doi.org/10.1128/ecosalplus.4.4.2.
16. McHenry CS. 2011. Bacterial replicases and related polymerases. Curr Opin Chem Biol 15:587–594. https://doi.org/10.1016/j.cbpa.2011.07.018.

17. Maki S, Kornberg A. 1988. DNA polymerase III holoenzyme of *Escherichia coli*. III. Distinctive processive polymerases reconstituted from purified subunits. J Biol Chem 263:6561–6569. https://doi.org/10.1016/S0021-9258(18)68678-8.
18. Studwell PS, O'Donnell M. 1990. Processive replication is contingent on the exonuclease subunit of DNA polymerase III holoenzyme. J Biol Chem 265:1171–1178. https://doi.org/10.1016/S0021-9258(19)40174-9.
19. Toste Rego A, Holding AN, Kent H, Lamers MH. 2013. Architecture of the Pol III-clamp-exonuclease complex reveals key roles of the exonuclease subunit in processive DNA synthesis and repair. EMBO J 32:1334–1343. https://doi.org/10.1038/emboj.2013.68.
20. Jergic S, Horan NP, Elshenawy MM, Mason CE, Urathamakul T, Ozawa K, Robinson A, Goudsmits JM, Wang Y, Pan X, Beck JL, van Oijen AM, Huber T, Hamdan SM, Dixon NE. 2013. A direct proofreader-clamp interaction stabilizes the Pol III replicase in the polymerization mode. EMBO J 32:1322–1333. https://doi.org/10.1038/emboj.2012.347.
21. Naktinis V, Onrust R, Fang L, O'Donnell M. 1995. Assembly of a chromosomal replication machine: two DNA polymerases, a clamp loader, and sliding clamps in one holoenzyme particle. II. Intermediate complex between the clamp loader and its clamp. J Biol Chem 270:13358–13365. https://doi.org/10.1074/jbc.270.22.13358.
22. Lopez de Saro FJ, O'Donnell M. 2001. Interaction of the beta sliding clamp with MutS, ligase, and DNA polymerase I. Proc Natl Acad Sci U S A 98:8376–8380. https://doi.org/10.1073/pnas.121009498.
23. Bonner CA, Stukenberg PT, Rajagopalan M, Eritja R, O'Donnell M, McEntee K, Echols H, Goodman MF. 1992. Processive DNA synthesis by DNA polymerase II mediated by DNA polymerase III accessory proteins. J Biol Chem 267:11431–11438. https://doi.org/10.1016/S0021-9258(19)49928-6.
24. Hughes AJ, Jr., Bryan SK, Chen H, Moses RE, McHenry CS. 1991. *Escherichia coli* DNA polymerase II is stimulated by DNA polymerase III holoenzyme auxiliary subunits. J Biol Chem 266:4568–4573. https://doi.org/10.1016/S0021-9258(20)64360-5.
25. Sutton MD, Opperman T, Walker GC. 1999. The *Escherichia coli* SOS mutagenesis proteins UmuD and UmuD' interact physically with the replicative DNA polymerase. Proc Natl Acad Sci U S A 96:12373–12378. https://doi.org/10.1073/pnas.96.22.12373.
26. Dalrymple BP, Kongsuwan K, Wijffels G, Dixon NE, Jennings PA. 2001. A universal protein-protein interaction motif in the eubacterial DNA replication and repair systems. Proc Natl Acad Sci U S A 98:11627–11632. https://doi.org/10.1073/pnas.191384398.
27. Pluciennik A, Burdett V, Lukianova O, O'Donnell M, Modrich P. 2009. Involvement of the beta clamp in methyl-directed mismatch repair *in vitro*. J Biol Chem 284:32782–32791. https://doi.org/10.1074/jbc.M109.054528.
28. Kato J, Katayama T. 2001. Hda, a novel DnaA-related protein, regulates the replication cycle in *Escherichia coli*. EMBO J 20:4253–4262. https://doi.org/10.1093/emboj/20.15.4253.
29. Sutton MD, Narumi I, Walker GC. 2002. Posttranslational modification of the *umuD*-encoded subunit of *Escherichia coli* DNA polymerase V regulates its interactions with the beta processivity clamp. Proc Natl Acad Sci U S A 99:5307–5312. https://doi.org/10.1073/pnas.082322099.
30. Ozaki S, Matsuda Y, Keyamura K, Kawakami H, Noguchi Y, Kasho K, Nagata K, Masuda T, Sakiyama Y, Katayama T. 2013. A replicase clamp-binding dynamin-like protein promotes colocalization of nascent DNA strands and equipartitioning of chromosomes in *E. coli*. Cell Rep 4:985–995. https://doi.org/10.1016/j.celrep.2013.07.040.
31. Grigorian AV, Lustig RB, Guzman EC, Mahaffy JM, Zyskind JW. 2003. *Escherichia coli* cells with increased levels of DnaA and deficient in recombinational repair have decreased viability. J Bacteriol 185:630–644. https://doi.org/10.1128/JB.185.2.630-644.2003.
32. Babu VM, Sutton MD. 2014. A *dnaN* plasmid shuffle strain for rapid *in vivo* analysis of mutant *Escherichia coli* beta clamps provides insight into the role of clamp in *umuDC*-mediated cold sensitivity. PLoS One 9:e98791. https://doi.org/10.1371/journal.pone.0098791.
33. Sutton MD, Farrow MF, Burton BM, Walker GC. 2001. Genetic interactions between the *Escherichia coli umuDC* gene products and the beta processivity clamp of the replicative DNA polymerase. J Bacteriol 183:2897–2909. https://doi.org/10.1128/JB.183.9.2897-2909.2001.
34. Jeruzalmi D, Yurieva O, Zhao Y, Young M, Stewart J, Hingorani M, O'Donnell M, Kuriyan J. 2001. Mechanism of processivity clamp opening by the delta subunit wrench of the clamp loader complex of *E. coli* DNA polymerase III. Cell 106:417–428. https://doi.org/10.1016/S0092-8674(01)00462-7.
35. Naktinis V, Turner J, O'Donnell M. 1996. A molecular switch in a replication machine defined by an internal competition for protein rings. Cell 84:137–145. https://doi.org/10.1016/S0092-8674(00)81000-4.
36. Fernandez-Leiro R, Conrad J, Scheres SH, Lamers MH. 2015. cryo-EM structures of the *E. coli* replicative DNA polymerase reveal its dynamic interactions with the DNA sliding clamp, exonuclease and tau. Elife 4:e11134. https://doi.org/10.7554/eLife.11134.
37. Kim DR, McHenry CS. 1996. Identification of the beta-binding domain of the alpha subunit of *Escherichia coli* polymerase III holoenzyme. J Biol Chem 271:20699–20704. https://doi.org/10.1074/jbc.271.34.20699.
38. Dohrmann PR, McHenry CS. 2005. A bipartite polymerase-processivity factor interaction: only the internal beta binding site of the alpha subunit is required for processive replication by the DNA polymerase III holoenzyme. J Mol Biol 350:228–239. https://doi.org/10.1016/j.jmb.2005.04.065.
39. Duzen JM, Walker GC, Sutton MD. 2004. Identification of specific amino acid residues in the *E. coli* beta processivity clamp involved in interactions with DNA polymerase III, UmuD and UmuD'. DNA Repair (Amst) 3:301–312. https://doi.org/10.1016/j.dnarep.2003.11.008.
40. Sutton MD. 2004. The *Escherichia coli dnaN159* mutant displays altered DNA polymerase usage and chronic SOS induction. J Bacteriol 186:6738–6748. https://doi.org/10.1128/JB.186.20.6738-6748.2004.
41. Sutton MD, Duzen JM. 2006. Specific amino acid residues in the beta sliding clamp establish a DNA polymerase usage hierarchy in *Escherichia coli*. DNA Repair (Amst) 5:312–323. https://doi.org/10.1016/j.dnarep.2005.10.011.
42. Maul RW, Ponticelli SK, Duzen JM, Sutton MD. 2007. Differential binding of *Escherichia coli* DNA polymerases to the beta-sliding clamp. Mol Microbiol 65:811–827. https://doi.org/10.1111/j.1365-2958.2007.05828.x.
43. Kaguni JM, Kornberg A. 1984. Replication initiated at the origin (*oriC*) of the *E. coli* chromosome reconstituted with purified enzymes. Cell 38:183–190. https://doi.org/10.1016/0092-8674(84)90539-7.
44. Scouten Ponticelli SK, Duzen JM, Sutton MD. 2009. Contributions of the individual hydrophobic clefts of the *Escherichia coli* beta sliding clamp to clamp loading, DNA replication and clamp recycling. Nucleic Acids Res 37:2796–2809. https://doi.org/10.1093/nar/gkp128.
45. Sassanfar M, Roberts JW. 1990. Nature of the SOS-inducing signal in *Escherichia coli*. The involvement of DNA replication. J Mol Biol 212:79–96. https://doi.org/10.1016/0022-2836(90)90306-7.
46. Mukherjee A, Cao C, Lutkenhaus J. 1998. Inhibition of FtsZ polymerization by SulA, an inhibitor of septation in *Escherichia coli*. Proc Natl Acad Sci U S A 95:2885–2890. https://doi.org/10.1073/pnas.95.6.2885.
47. Trusca D, Scott S, Thompson C, Bramhill D. 1998. Bacterial SOS checkpoint protein SulA inhibits polymerization of purified FtsZ cell division protein. J Bacteriol 180:3946–3953. https://doi.org/10.1128/JB.180.15.3946-3953.1998.
48. Gaubig LC, Waldminghaus T, Narberhaus F. 2011. Multiple layers of control govern expression of the *Escherichia coli ibpAB* heat-shock operon. Microbiology (Reading) 157:66–76. https://doi.org/10.1099/mic.0.043802-0.
49. Gallegos MT, Schleif R, Bairoch A, Hofmann K, Ramos JL. 1997. Arac/XylS family of transcriptional regulators. *Microbiol Mol Biol Rev* 61:393–410. https://doi.org/10.1128/mmbr.61.4.393-410.1997.
50. Steen HB, Boye E. 1980. Bacterial growth studied by flow cytometry. Cytometry 1:32–36. https://doi.org/10.1002/cyto.990010108.
51. Skarstad K, Steen HB, Boye E. 1983. Cell cycle parameters of slowly growing *Escherichia coli* B/r studied by flow cytometry. J Bacteriol 154:656–662. https://doi.org/10.1128/jb.154.2.656-662.1983.
52. Boye E, Steen HB, Skarstad K. 1983. Flow cytometry of bacteria: a promising tool in experimental and clinical microbiology. J Gen Microbiol 129:973–980. https://doi.org/10.1099/00221287-129-4-973.
53. Bjedov I, Dasgupta CN, Slade D, Le Blastier S, Selva M, Matic I. 2007. Involvement of *Escherichia coli* DNA polymerase IV in tolerance of cytotoxic alkylating DNA lesions in vivo. Genetics 176:1431–1440. https://doi.org/10.1534/genetics.107.072405.
54. Maul RW, Sutton MD. 2005. Roles of the *Escherichia coli* RecA protein and the global SOS response in effecting DNA polymerase selection in vivo. J Bacteriol 187:7607–7618. https://doi.org/10.1128/JB.187.22.7607-7618.2005.
55. Heltzel JM, Maul RW, Wolff DW, Sutton MD. 2012. *Escherichia coli* DNA polymerase IV (Pol IV), but not Pol II, dynamically switches with a stalled Pol III* replicase. J Bacteriol 194:3589–3600. https://doi.org/10.1128/JB.00520-12.
56. Viguera E, Petranovic M, Zahradka D, Germain K, Ehrlich DS, Michel B. 2003. Lethality of bypass polymerases in *Escherichia coli* cells with a defective clamp loader complex of DNA polymerase III. Mol Microbiol 50:193–204. https://doi.org/10.1046/j.1365-2958.2003.03658.x.
57. Ozawa K, Horan NP, Robinson A, Yagi H, Hill FR, Jergic S, Xu ZQ, Loscha KV, Li N, Tehei M, Oakley AJ, Otting G, Huber T, Dixon NE. 2013.

Proofreading exonuclease on a tether: the complex between the *E. coli* DNA polymerase III subunits alpha, epsilon, theta and beta reveals a highly flexible arrangement of the proofreading domain. Nucleic Acids Res 41:5354–5367. https://doi.org/10.1093/nar/gkt162.
58. Babu VMP, Homiski C, Scotland MKSC, Kaguni JM, Sutton MD. 2021. Elevated levels of the *E. coli nrdAB*-encoded ribonucleotide reductase counteracts the toxicity caused by an increased abundance of the beta clamp. *J Bacteriol*
59. Leu FP, Hingorani MM, Turner J, O'Donnell M. 2000. The delta subunit of DNA polymerase III holoenzyme serves as a sliding clamp unloader in *Escherichia coli*. J Biol Chem 275:34609–34618. https://doi.org/10.1074/jbc.M005495200.
60. Sutton MD, Duzen JM, Maul RW. 2005. Mutant forms of the *Escherichia coli* beta sliding clamp that distinguish between its roles in replication and DNA polymerase V-dependent translesion DNA synthesis. Mol Microbiol 55:1751–1766. https://doi.org/10.1111/j.1365-2958.2005.04500.x.
61. Babu VMP, Itsko M, Baxter JC, Schaaper RM, Sutton MD. 2017. Insufficient levels of the *nrdAB*-encoded ribonucleotide reductase underlie the severe growth defect of the Deltahda *E. coli* strain. Mol Microbiol 104:377–399. https://doi.org/10.1111/mmi.13632.
62. Fujimitsu K, Su'etsugu M, Yamaguchi Y, Mazda K, Fu N, Kawakami H, Katayama T. 2008. Modes of overinitiation, *dnaA* gene expression, and inhibition of cell division in a novel cold-sensitive *hda* mutant of *Escherichia coli*. J Bacteriol 190:5368–5381. https://doi.org/10.1128/JB.00044-08.
63. Herrick J, Sclavi B. 2007. Ribonucleotide reductase and the regulation of DNA replication: an old story and an ancient heritage. Mol Microbiol 63:22–34. https://doi.org/10.1111/j.1365-2958.2006.05493.x.
64. Bunting KA, Roe SM, Pearl LH. 2003. Structural basis for recruitment of translesion DNA polymerase Pol IV/DinB to the beta-clamp. EMBO J 22:5883–5892. https://doi.org/10.1093/emboj/cdg568.
65. Heltzel JM, Maul RW, Scouten Ponticelli SK, Sutton MD. 2009. A model for DNA polymerase switching involving a single cleft and the rim of the sliding clamp. Proc Natl Acad Sci U S A 106:12664–12669. https://doi.org/10.1073/pnas.0903460106.
66. Fuller RS, Kaguni JM, Kornberg A. 1981. Enzymatic replication of the origin of the *Escherichia coli* chromosome. Proc Natl Acad Sci U S A 78:7370–7374. https://doi.org/10.1073/pnas.78.12.7370.
67. Kelman Z, Yao N, O'Donnell M. 1995. *Escherichia coli* expression vectors containing a protein kinase recognition motif, His6-tag and hemagglutinin epitope. Gene 166:177–178. https://doi.org/10.1016/0378-1119(95)00556-7.
68. Bradford MM. 1976. A rapid and sensitive method for the quantitation of microgram quantities of protein utilizing the principle of protein-dye binding. Anal Biochem 72:248–254. https://doi.org/10.1006/abio.1976.9999.
69. Karlsson R, Katsamba PS, Nordin H, Pol E, Myszka DG. 2006. Analyzing a kinetic titration series using affinity biosensors. Anal Biochem 349:136–147. https://doi.org/10.1016/j.ab.2005.09.034.
70. Andersson K, Hamalainen M, Malmqvist M. 1999. Identification and optimization of regeneration conditions for affinity-based biosensor assays. A multivariate cocktail approach. Anal Chem 71:2475–2481. https://doi.org/10.1021/ac981271j.
71. Myszka DG, Morton TA. 1998. CLAMP: a biosensor kinetic data analysis program. Trends Biochem Sci 23:149–150. https://doi.org/10.1016/s0968-0004(98)01183-9.
72. Datsenko KA, Wanner BL. 2000. One-step inactivation of chromosomal genes in *Escherichia coli* K-12 using PCR products. Proc Natl Acad Sci U S A 97:6640–6645. https://doi.org/10.1073/pnas.120163297.
73. Baxter JC, Sutton MD. 2012. Evidence for roles of the *Escherichia coli* Hda protein beyond regulatory inactivation of DnaA. Mol Microbiol 85:648–668. https://doi.org/10.1111/j.1365-2958.2012.08129.x.
74. Johnsen L, Flatten I, Morigen Dalhus B, Bjoras M, Waldminghaus T, Skarstad K. 2011. The G157C mutation in the *Escherichia coli* sliding clamp specifically affects initiation of replication. Mol Microbiol 79:433–446. https://doi.org/10.1111/j.1365-2958.2010.07453.x.
75. Sanders LH, Devadoss B, Raja GV, O'Connor J, Su S, Wozniak DJ, Hassett DJ, Berdis AJ, Sutton MD. 2011. Epistatic roles for *Pseudomonas aeruginosa* MutS and DinB (DNA Pol IV) in coping with reactive oxygen species-induced DNA damage. PLoS One 6:e18824. https://doi.org/10.1371/journal.pone.0018824.
76. Scotland MK, Heltzel JM, Kath JE, Choi JS, Berdis AJ, Loparo JJ, Sutton MD. 2015. A genetic selection for *dinB* mutants reveals an interaction between DNA polymerase IV and the replicative polymerase that is required for translesion synthesis. PLoS Genet 11:e1005507. https://doi.org/10.1371/journal.pgen.1005507.
77. Edgar R, Domrachev M, Lash AE. 2002. Gene Expression Omnibus: NCBI gene expression and hybridization array data repository. Nucleic Acids Res 30:207–210. https://doi.org/10.1093/nar/30.1.207.
78. Wang RF, Kushner SR. 1991. Construction of versatile low-copy-number vectors for cloning, sequencing and gene expression in *Escherichia coli*. Gene 100:195–199. https://doi.org/10.1016/0378-1119(91)90366-J.